

**Study of fracture toughness of Zr-2.5Nb alloy  
used in pressure tube of Indian PHWR having  
more than 200 wppm hydrogen**

**M.Tech. Thesis**

**By**

**PRATIK PARAG GHADSE**



**DEPARTMENT OF METALLURGY ENGINEERING  
AND MATERIAL SCIENCE**

**INDIAN INSTITUTE OF TECHNOLOGY  
INDORE**

**June, 2020**

**Study of fracture toughness of Zr-2.5Nb alloy  
used in pressure tube of Indian PHWR having  
more than 200 wppm hydrogen**

**A THESIS**

*Submitted in partial fulfillment of the  
Requirements for the award of the degree  
of*

**Master of Technologic**

**By**

**PRATIK PARAG GHADSE**



**DEPARTMENT OF METALLURGY ENGINEERING  
AND MATERIAL SCIENCE**

**INDIAN INSTITUTE OF TECHNOLOGY  
INDORE**

**June, 2020**



# INDIAN INSTITUTE OF TECHNOLOGY INDORE

## CANDIDATE'S DECLARATION

I hereby certify that, the work which is being presented in the thesis entitled "Study of fracture toughness of Zr-2.5Nb alloy used in pressure tube of Indian PHWR having more than 200 wppm hydrogen" in the partial fulfillment of the requirements for the award of the degree of MASTER OF TECHNOLOGY in METALLURGY ENGINEERING and submitted in the DEPARTMENT OF METALLURGY ENGINEERING AND MATERIAL SCIENCE, Indian Institute of Technology Indore, is an authentic record of my own work carried out during the time period From August, 2018 to June, 2020 under the supervision of Dr. Vinod Kumar, METALLURGY ENGINEERING AND MATERIAL SCIENCE, INDIAN INSTITUTE OF TECHNOLOGY INDORE

The matter presented in this thesis has not been submitted by me for the award of any other degree of this or any other institute.

*Pratik Parag Ghadse*  
20/06/20

**Pratik Parag Ghadse**

This is to certify that the above statement made by the candidate is correct to the best of my Knowledge.

**Dr. Vinod Kumar**

**Supervisor of M.Tech. Thesis**

**PRATIK PARAG GHADSE** has successfully given his/her M.Tech. Oral Examination held on

**Supervisor(s) of M.Tech. Thesis.**

**Convener, DPGC**

**Date:**

**Date:**

*K. Eswara murugan*  
29/6/2020

*M. Jayaprakash*

**Dr. Eswara Korimilli**

**Dr. Jayaprakash Murugesan**

**PSPC Member #1**

**PSPC Member #2**

**Date: 29/06/20**

**Date: 29/06/20**

## ACKNOWLEDGEMENTS

*I would like to thank Dr. R. N. Singh, Head of Mechanical Metallurgy Division BARC, for accepting me under him without whom this thesis would not be possible. Dr. A. K. Bind and Dr. A. Gopalan for their constant help and support during this project. Thank you sir Dr. Vinod Kumar, HOD Of MEMS, IIT Indore, for his guidance and believing in me that I can perform my project in BARC. Thank you sir Dr. Eswara Korimilli and Dr. Jayaprakash Murugesan , PSPC Member IIT Indore, for your comments and reviews and pointing out my mistakes and directing me towards correct direction. I would also like to give special thanks to all my batch mate and all the good friends I made during my M.Tech in IIT Indore and to IIT Indore for this last two years. Finally I would like to thank HRDD Department BARC for providing an opportunity to work and also to whole BARC for providing facility to perform project.*

## Abstract

Due to chemical reaction between heavy water and Zr-2.5 alloy pressure tube (PT) material, hydrogen is released which get absorbed by PT. The hydrogen in excess of terminal solid solubility precipitate out in the form of brittle Zirconium hydride. The hydrides are of platelet shape and may get oriented in normal direction to the applied hoop stress above threshold stress value. Stress reoriented hydrides in the radial axial plane are called as radial hydrides and can cause severe embrittlement in PT.

This study was done to evaluate the fracture toughness of CWSR Zr-2.5Nb pressure tube containing more than 200wppm hydrogen oriented in radial direction. The charging of a pressure tube spool was done by gaseous hydrogen charging in constant volume. After hydrogen is charged into the pressure tube spool, circumferential hydrides are formed. The Circumferential hydrides are reoriented into radial hydride using a setup to pressurize the tube from internally at 350°C, so that the hoop stress developed into the spool will be greater than threshold stress value. The cooling from 300°C to 150°C at constant pressure above threshold value will reorient the hydride in radial direction.

Curved compact specimen of 17 mm width was machined using wire electric discharge machining from a CWSR Zr-2.5Nb pressure tube spool of Indian pressurized heavy water reactor. Metallographic examination of each sample shows 100% radial hydrides. The specimen where pre-cracked and then tested between the temperature range from 25°C to 300°C. The fracture toughness of sample was calculated as per standard ASTM E1820-13. The fracture toughness versus temperature graph shows clear brittle to ductile transition. Fracture toughness reaches 207 KJ/m<sup>2</sup> at 300°C, where as at room temperature the fracture toughness is 3 KJ/m<sup>2</sup>.

## TABLE OF CONTENTS

	Page No
LIST OF FIGURES.	VII
LIST OF TABLES.	IX
NOMENCLATURE.	X
Chapter 1: Introduction.	1
Chapter 2: Literature Review.	7
Chapter 3: Material and Method.	16
3.1: Material Specification.	16
3.2: Hydrogen Charging.	18
3.3: Radial Hydride Formation.	20
3.4: Pre-Cracking.	21
3.5: Experimentation.	23
3.6: Pre-Crack Length Calculation.	25
3.7: Metallographic Analysis.	26
3.8: Hydrogen Content Analysis.	29
3.9: Fracture Toughness Analysis.	30
3.10: Critical Crack Length Analysis.	36
Chapter 4: Result And Discussion.	34
Chapter 5: Conclusions.	46
Chapter 6: Future Direction	47
REFERENCES.	48

## LIST OF FIGURES

Fig 1 <sup>st</sup> . A schematic representation of PHWR.	1
Fig 2 Schematic representation of grain size in PT.	4
Fig.3.a. Zr-H phase diagram from[26].	6
Fig.3.b. Zr-Nb phase diagram.[33].	6
Fig.4. Step wise representation of manufacturing of pressure tube in NFC Hyderabad according to Modified AECL route 2 of Indian standard.	17
Fig.5.a. CCT sample cut from PT spool .	21
Fig.5.b. CCT sample specification and dimensions.	21
Fig 6. UTM Zwick Roell Kappa 100DS.	24
Fig 7. Optical microscope image of RC plane for test temperature 300°C.	26
Fig 8. Optical microscope image of RC plane for test temperature 275°C.	26
Fig 9. Optical microscope image of RC plane for test temperature 262°C.	27
Fig 10. Optical microscope image of RC plane for test temperature 250°C.	27
Fig 11. Optical microscope image of RC plane for test temperature 225°C.	27
Fig 12. Optical microscope image of RC plane for test temperature 150°C.	28
Fig 13. Optical microscope image of RC plane for test temperature 25°C.	28
Fig.14. Load vs Load Line Displacement vs DCPD graph for test temperature 300°C.	32
Fig.15. Load vs Load Line Displacement vs DCPD graph for test temperature 275°C.	32
Fig.16. Load vs Load Line Displacement vs DCPD	

graph for test temperature 262°C.	33
Fig.17. Load vs Load Line Displacement vs DCPD graph for test temperature 250°C.	33
Fig.18. Load vs Load Line Displacement vs DCPD graph for test temperature 225°C.	34
Fig.19. Load vs Load Line Displacement vs DCPD graph for test temperature 150°C.	34
Fig.20. Load vs Load Line Displacement vs DCPD graph for test temperature 25°C.	35
Fig.21. Load vs Load Line Displacement vs higher magnification of DCPD graph for test temperature 25°C.	35
Fig.22. Load vs. load line displacement for all temperature range.	39
Fig.23. Front and back surface of CCT sample for ductile and brittle test sample.	40
Fig.24. Stereo microscope image of crack surface after fracture testing for test temperature 300°C.	40
Fig.25. Stereo microscope image of crack surface after fracture testing for test temperature 275°C.	41
Fig.26. Stereo microscope image of crack surface after fracture testing for test temperature 262°C.	41
Fig.27. Stereo microscope image of crack surface after fracture testing for test temperature 250°C.	42
Fig.28. Stereo microscope image of crack surface after fracture testing for test temperature 225°C.	42
Fig.29. Stereo microscope image of crack surface after fracture testing for test temperature 150°C.	43
Fig.30. Stereo microscope image of crack surface after fracture testing for test temperature 25°C.	43
Fig.31. J <sub>max</sub> vs. temperature for more than 200 wppm radial hydride, along with comparison for unhydrided, 100 wppm circumferential hydrided and 200 wppm circumferentially hydrided taken from [2].	44
Fig.32. CCL vs Test Temperature for uncharged Zr-2.5Nb from [2], LLB crack length with factor of safety and for radial hydride having more than 200wppm hydrogen.	44
Fig.33. Graph of terminal solid solubility of dissolution verses temperature.[16]	45



## **LIST OF TABLES**

1) Table 1.Composition of double melted and quadruple melted pressure tube .	16
2) Table 2. Fracture Toughness and CCL calculation data.	45

## NOMENCLATURE

AGMS	Annulus Gas Monitoring System
ASTM	American Society for Testing and Materials
$\Delta a$	Crack growth
CCL	Critical Crack Length
CCT	Curved Compact Tension
CWSR	Cold Worked and Stress Relieved
DCPD	Direct Current Potential Drop
EDM	Electro-Discharge Machining
HCC	Hydride Continuity Coefficient
$J_{max}$	J value corresponding to maximum load
LLB	Leak Before Break
PHWR	Pressurized Heavy Water Reactor
PT	Pressure Tube
wppm	Part per million in weight
RT	Room Temperature
RA	Radial- Axial
RC	Radial Circumferential
AC	Axial Circumferential

## Chapter 1

### Introduction

Indian pressurized heavy water reactor (PHWR) consists of fuel rods, pressure tubes, calandria tubes, moderator tank, garter spring and other peripheral component. The fuel rods are consists of nuclear fuel inside. The pressure tube surrounds the fuel rod. The calendar tube surrounds the pressure tube and houses an inert gas between calandria tube and pressure tube and finally it is surrounded by moderator.

The pressurized heavy water reactor uses the heat generated during nuclear reaction to increase the temperature of primary circulating hot coolant to transfer heat to the secondary circulating water. The secondary water is converted to steam to generate electricity. The primary circulating coolant flow through PT shown in figure.1

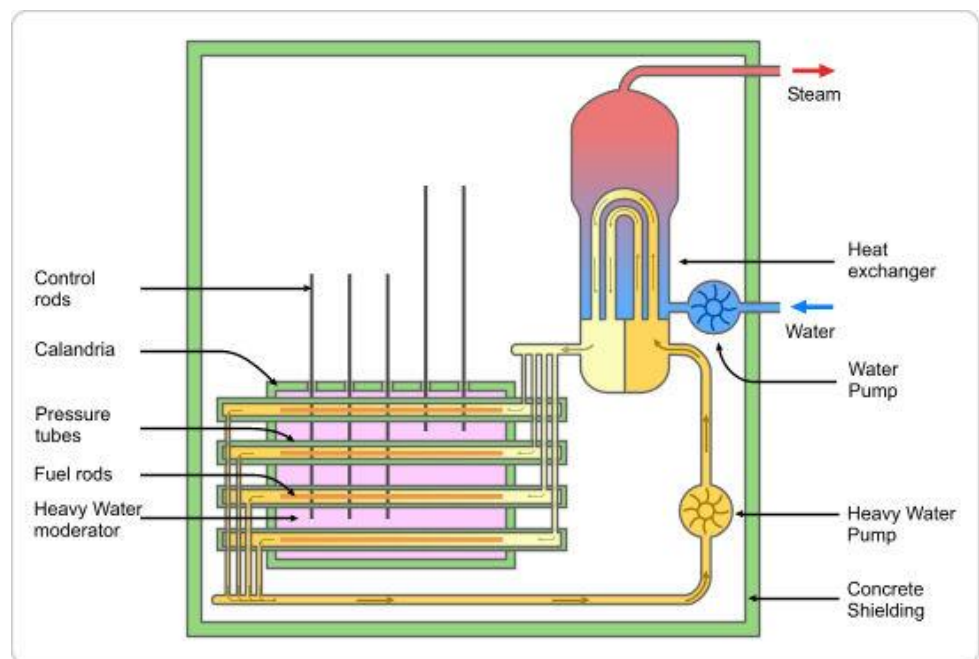


Fig 1<sup>st</sup>. A schematic representation of PHWR.

The reactor demand that the various core structural element of the PHWR such as cladding tube, pressure tube, calandria tube, spring must have low neutron absorption cross section and should satisfy the physical, mechanical, metallurgical and chemical requirement of radiation environment. Apart from satisfying the generic requirement of

the nuclear structural material like good corrosion resistance and adequate high temperature strength and ductility under operating condition, Zr alloy meet the specific requirement of the nuclear structural material.

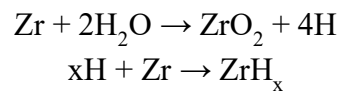
Zr alloy have low neutron absorption cross section, high melting point, adequate high temperature strength, acceptable corrosion resistance in aqueous medium, good fabricability and weldability, microstructure and irradiation stability, that's why it is used for various core structure element in a nuclear reactor. Pressure tube being the primary boundary containment for the hot coolant is made of Zirconium 2.5 Niobium and houses fuel rods. Pressure tubes are exposed to heavy water coolant flowing through it under a pressure of around 10 MPa, temperature in the range of 250 to 300 °C and fast neutron flux of  $3 \times 10^{17} \text{ n/m}^2\text{s}$ . [20]

Zr-2.5Nb alloy satisfied all the nuclear structural requirement of pressure tube. Pressure tube being the primary boundary for the containment of pressurized hot heavy water coolant in PHWR their integrity is to be maintained during reactor operation.

The pressure tube is exposed to irradiation, stress and corrosion, high temperature environment, which result in change in mechanical property, chemical composition and microstructure. Because of that they are subjected to various deteriorating effects such as blister, creep, crack, hydrogen embrittlement, microstructure degradation, DHC. All this factors are life limiting for PT. A postulated loss of coolant accident (loca), in which primary coolant fail to remove the heat from the core, temperature and pressure of the tube will rise very quickly.

Hydrogen embrittlement is one of the major reason which leads to the failure of PT. In different countries different fabrication route are employed such as cold work and annealed in Russia. Canada employs cold work and stress relieved and Russia uses water quenched and aged. In conventional route the extrusion ratio of 11:1 is employed followed by cold drawing 20%. Later AECL developed modified route for improved in reactor performance. The modified route has an excursion ratio of 8:1. The Indian PT fabrication route is similar to AECL modified route but not same. The AECL modified route consists of two cold working steps of 20% each with an intermediate annealing at 923 Kelvin for half hour. For Indian PT made, followed at nuclear fuel complex impart 50-55% large cold working for the first stage followed by a process called pilgering which imparts simultaneous reduction of wall thickness and diameter[24].

This route produces strong structure of elongated  $\alpha$  grain which is surrounded by very thin nearly continuous  $\beta$  phase network along the grain boundaries. The Basal pole predominantly oriented along 54% in circumferential direction, 43% in radial direction and 3% in axial direction due to the fabrication route. The habit plane for the growth of hydrides platelet is oriented  $\sim 14$  degree to the basal plane[20]. The initial hydrogen content is kept as minimum as possible. For a quadruple melted less than 5 wppm.



The above chemical reaction between heavy water and Zirconium produces hydrogen which gets absorbed in the Zr matrix and form hydrides if the concentration of hydrogen is more than the terminal solid solubility. The hydrogen greater than the terminal solid solubility precipitate out as  $\gamma$ ,  $\delta$  and  $\varepsilon$  hydride. However under the reaction operating condition and cooling rate only  $\delta$  hydride precipitate [26]. This  $\delta$  hydride has platelet like morphology. The nucleation and growth of

hydride is stacked parallel to the basal plane of the  $\alpha$ -Zr and starts at the  $\alpha/\beta$  interface as the hydride platelet has singular orientation, it eventually grows and coalescence into the structure according to the texture of Zr-2.5Nb pressure tube that is along circumferential axial direction under unstressed condition [21]. Under a stressed condition with stress greater than the threshold stress the hydride forms perpendicular to the direction of tensile force. Below shows a graphical representation of dimensions of grain in pressure tube. [26]

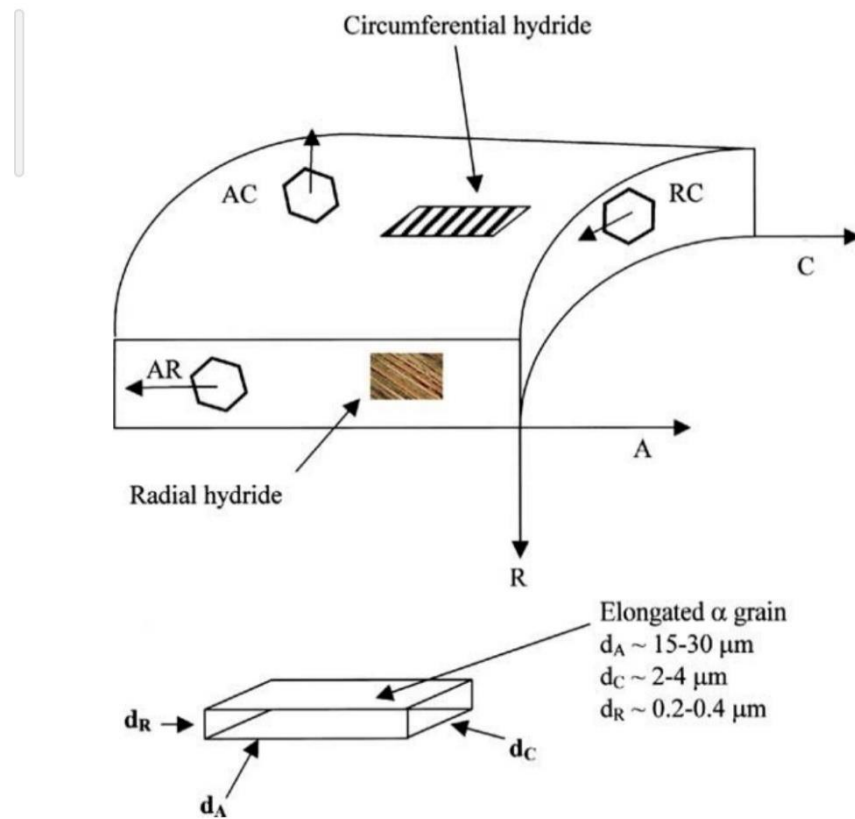


Fig 2 schematic representation of grain size in PT.[2]

## Chapter 2

### Literature Review

Adequate high temperature, aqueous corrosion resistance, low neutron absorption cross section, microstructure stability due to radiation these are some of the general requirement of a nuclear plant material. That's why Zirconium alloy is extensively used in nuclear application [2].

In earlier days two alloys of Zirconium i.e. Zircaloy-2 and Zircaloy-4 are extensively used in nuclear industry. Their composition are [Zircaloy-2 (Zr-1.5Sn-0.12Fe-0.1Cr-0.05Ni in wt%) and Zircaloy-4 (Zr-1.5Sn-0.2Fe-0.1Cr-0.007Ni in wt%)] [31]. One other composition of Zirconium alloy Zr-2.5Nb-0.5Cu is used for garter spring [26]. Earlier generation reactor uses Zircaloy 2 and 4 for boiling water reactor, pressurized water reactor and CANDU uses Zircaloy-4 for fuel cladding.

Earlier, in CANDU reactor Zircaloy-2 was used for pressure tube but now they use Zr-2.5Nb alloy pressure tubes. It was found that the hydrogen terminal solid solubility for Zr-2.5Nb is more than Zr. The terminal solid solubility due to addition of Tin is higher than Zr-2.5Nb but contradict to that the hydrogen pickup capacity of Zircaloy-2 and Zircaloy-4 is higher than Zr-2.5Nb alloy. That's why Zircaloy-2 is replaced by Zirconium 2.5 Niobium in pressure tube [26]. The addition of Niobium in the Zirconium makes the  $\beta$  phase stable. According to author, addition of alloying element niobium, nickel, vanadium, titanium decreases the stability of hydrogen in both the  $\beta$  and  $\alpha$  phase of Zr-2.5Nb, but hydrogen pickup rate also decreases [26]. Therefore, for better in reactor performance, Zircaloy with main alloying element as tin was replaced by Zr-2.5Nb as a material suitable for pressure tube [24]. According to [16] the Niobium acts as a  $\beta$ -phase stabilizer and contain 10 to 20% Nb volume in BCC structure. Niobium also increases creep resistance. New developed Zr alloy for cladding such as ZIRLO (Zr-1.1Sn-0.11Fe-1.2Nb) and M5 (Zr-0.04Fe-1.0Nb) are more resistant to corrosion and hydrogen pickup compared to Zircaloy-2 and Zircaloy-4

[31]. The Zr-H phase diagram from [26] shows three phases of Zr-H i.e.  $\gamma$ ,  $\delta$  and  $\epsilon$ . But due to temperature and concentration of hydrogen in Zr only  $\delta$  hydride precipitate and has a crystal structure of FCC.

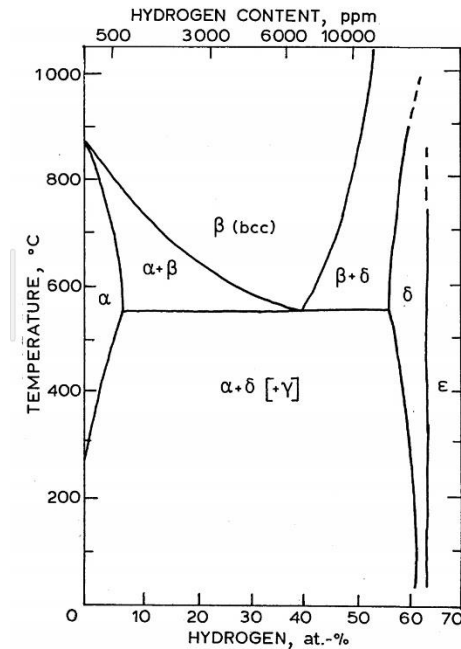


Fig.3.a. Zr-H phase diagram from[26]

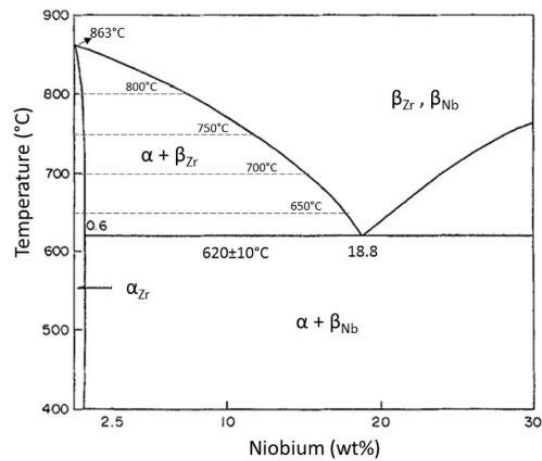


Fig.3.b. Zr-Nb phase diagram.[33]

Hydrogen embrittlement is a major life limiting factor. In pressure tube hydrogen form hydride which is brittle nature and results in making the Zr matrix brittle. Under normal operating condition the hydrogen pickup is 1wppm per year during it's 30 years of life, but under



abnormal conditions the corrosion reaction may escalates and the pickup rate may increase exponentially [16].

In PT the hoop to axial stress is 2: 1. As the circumferential hydrate plates form parallel to the hoop stress the embrittlement effect due to this is less as compared to radial hydrides this is due to the fact that the surface perpendicular to the hoop stress contain less cross section area of hydrides. In radial hydrides the cross-section surface area coverage of the hydride is more. As the hydride platelet is perpendicular to the hoop stress which result in more significant embrittlement effect. Also due to the end to end surface joining of hydride in radial hydrides, through thickness crack forms along the radial hydride direction perpendicular to the hoop stress. The hydrogen embrittlement of PT material is enhanced by the presence of radial hydrides. In overall hydrogen embrittlement results in the decrease in the fracture toughness of pressure tube. That's why it is important to study the fracture toughness due to hydrogen embrittlement. Though the chemical composition of The Zr-2.5Nb alloy is nearly identical, the metallurgical condition of the Zr-2.5Nb tubes vary in different countries and hence in-service performance is also reported to vary [24].

Here follows some studies which are carried on Zi-2.5Nb pressure tube to understand terminal solid solubility, mechanical properties, reorientation stress, delayed hydride cracking and the nature of fracture.

- 1) Rishi K. Sharma et al [2]:-In this paper experimentation has done to calculate the fracture toughness for CWSR Zr – 2.5Nb pressure tube for both circumferential and radial hydride. The hydrogen charging was done by gas hydrogen charging up to 100 wppm. The first objective of the this study was to design an experimental setup where stress re-orientation of hydrides can be carried out on spool piece of Zr-2.5%Nb alloy pressure tube material. It reported a FT at 25°C 6.5 kJ/m<sup>2</sup> and at 300°C 204kJ/m<sup>2</sup>. The typical s shape of radial hydride Jmax vs

temperature curve can be seen at 225°C-250°C. In the SEM images of the sample, the cracked surface shows a flat region for 25 °C and pits and holes for 300 °C. It has been stated in this paper that terminal solid solubility is ~160 wppm at 400 °C to ~0.05 wppm at 20 °C.

- 2) Rishi K. Sharma et al [4]:-In this paper the effects of HCC on the fracture toughness of Zirconium 2.5 Niobium pressure tube has been studied. HCC, the hydrogen continuity coefficient which gives the fraction by which the hydrides are oriented in circumferential or radial direction. In the experimentation the spool was first charged with gas hydrogen charging up 100 ppm and then hoop stress is applied using a plunger to create radial hydrides. Some samples are annealed at 300°C, 325°C and 350°C. With the increasing annealing temperature the HCC decreases which shows that conversion of radial hydrides to circumferential hydrides. The conclusion is drawn that with the decrease in HCC, the transition temperature shifts toward lower temperature and higher fracture toughness.
- 3) G.D. Moan et al [6]:- In this the DHC velocity and its relation with the time available for the removal of pressure tube is studied. The study is done on CANDU pressure tube Zr-2.5Nb. It gives the optimum length of crack before which the leakage is not visible. It shows that the crack initiation starts from inside the tube and moves towards outside. The length of the crack LLB is 4 times the thickness of PT. After initiation of crack inside, the corrosion takes place in the crack and with each cycle the crack propagates. The threshold stress for DHC is 4.5-7 MPa√m.

- 4) R.N. Singh et al [7]:- In this work, influence of hydrogen and temperature on the fracture toughness parameters of unirradiated, cold worked and stress relieved CWSR Zr–2.5Nb pressure tube alloys used in Indian Pressurized Heavy Water Reactor is reported. The tests were carried on a 17 mm width CCT specimens machined from gaseous hydrogen charged tube-sections (21-90 ppm). Metallography of the sample shows circumferential hydride. Fracture toughness tests were carried out in the temperature range of 30–300°C as Per ASTM standard E-1820-06, DCPD technique was used to calculate crack length. The fracture toughness parameters ( $J_Q$ ,  $J_{max}$  and  $dJ/da$ ), were determined. It was reported that for a given test temperature, the fracture toughness parameters representing crack initiation ( $J_Q$ ) and crack propagation ( $J_{max}$ , and  $dJ/da$ ) is practically unaffected by hydrogen content. Also, for given hydrogen content, all the above mentioned fracture toughness parameters increased with temperature. CWSR Zr–2.5Nb, double melted unirradiated, pressure tube material having concentration range of 21–90 wppm is used. The fracture surface showed large number of CA-mesocracks normal to crack growth plane. The authors believe that fracture toughness parameters were not significantly affected with increase in hydrogen content from 21 to 90 wppm. Also, for a given hydrogen content crack initiation fracture toughness parameter showed weak temperature dependence whereas the crack propagation fracture toughness parameters increased with temperature to a saturation value.
- 5) K.S. Chan et al [8]:-In this study, in situ sem is done to determine the hydride reorientation stress for Zirconium alloy cladding materials containing circumferential hydrides and to characterize the fracture resistance of Zircaloy-2 after hydride reorientation. HRT heat treatment was performed on hydrogen-charged Zircaloy-2 specimens at 593 K or 623 K for 1 to 2 hours,

Followed by cooling to 473 K. Fracture testing was conducted on hydride-reoriented Three-point bend specimens at 473 K using an in situ loading stage inside a scanning electron microscope. Direct observations indicated that the reoriented hydrides, which ranged from – 1 to 22  $\mu\text{m}$  in lengths, were more prone to fracture at larger sizes ( $>10 \mu\text{m}$ ) compared to smaller sizes ( $<0.5 \mu\text{m}$ ). The reoriented hydrides reduced fracture resistance through a void nucleation, growth, and coalescence process at the crack tip. The resulting crack-resistance curves for Zircaloy-2 with reoriented hydrides decrease from 38 to 21  $\text{MPa}(\text{m})^{1/2}$  with increasing hydrogen contents from 51 to 1265 wt ppm hydrogen. The conclusions reached in this study are HRT occurs in Zircaloy-2 at stress intensity levels ranging from 5.5 to 27.4  $\text{MPa}(\text{m})^{1/2}$  and zone sizes of reorientation are found consistent with a stress level above 90 MPa. Reoriented hydrides formed in Zircaloy-2 ranged from submicron-sized to as large as 22  $\mu\text{m}$ . Fracture of reoriented hydrides of larger sizes ( $>10 \mu\text{m}$ ) is more widespread than that of smaller sizes ( $<5 \mu\text{m}$ ). Fracture toughness of Zircaloy-2 for 200°C decreases from 38 to 20  $\text{MPa}(\text{m})^{1/2}$  with increasing hydrogen content from 51 to 1256 wt ppm hydrogen. Zircaloy-2 exhibits a R curve fracture behavior at 473 K due to a combination of transformation toughening resulted from precipitation of reoriented hydrides and plastic blunting of the Zirconium ligaments.

- 6) Jun Cui et al [9]:-In this paper CANDU reactor Zr-2.5Nb alloy pressure tubes is studied. The paper presents an experimental study on the effect of hydride morphology and test temperature on axial fracture toughness of a cold-worked, unirradiated Zr-2.5Nb pressure tube. Compact tension specimens prepared from a section which was electrolytically hydride to 70 ppm hydrogen. Reoriented hydrides were formed using thermal cycles under an applied tensile hoop stress of 160 MPa. The hydride

morphologies were characterized by a parameter referred to as the hydride continuity coefficient of partially reoriented hydrides with HCC between 0.3-0.4 were formed under the stress and temperature cycle. J-R curves were generated to characterize the fracture behavior of the specimens tested at five different temperatures: 25°C (room temperature), 100°C, 150°C, 200°C and 250°C. Test results indicate that, for the as-received specimens, The fracture toughness is relatively high at room temperature and not significantly affected by the test temperature between room temperature and 250°C. For the 70 ppm hydrided specimens containing partially reoriented hydrides, the FT reported is significantly lower than that of the as-received specimens at room temperature. At 100°C, the fracture toughness is higher than that at room temperature but the average value is still lower than that of the as-received specimens. The specimens exhibit either brittle or ductile fracture behavior with a sharp transition to an upper-shelf toughness value. At 150°C, the specimens achieve an upper-shelf toughness level. Between 150°C and 250°C, the fracture toughness is similar to that of the as-received specimens and not affected by the reoriented hydrides.

- 7) R.N. Singh, et al [16]:- In this study terminal solid solubility of Zr-2.5Nb is calculated using dilatometry. Dilatometry is a method of identifying the change in dimension of material. When the material is charged with hydrogen it precipitates hydrides. When we heat the sample the hydride get dissolved back in to material which result in change in dimensions. The exponential function obtain from this study gives the terminal solid solubility wrt temperature. The study is done for Zr-2.5Nb PT material. The enthalpy and pre exponential term for dissolution and precipitation are given as (35.44, 63576.55) and (17.21, 3235.6). The paper states that the hysteresis in

dissolution and precipitation is due to tensile stress field developed during dissolution and compressive stress field during precipitation.

8) A.K. Bind, et al [17]:- In this paper, study influence of loading rate and hydrogen content on fracture toughness of Indian Zr-2.5Nb pressure tube containing less than 100wppm circumferential hydride is done. For the safety assessment of PHWR, it is required to study the flaw tolerance capacity of the pressure tubes as a function of the loading rate. For the as received material, the pulling rate only had an effect on fracture toughness at 25°C whereas for hydrided material the pulling rate affected fracture toughness in the transition regime. Hydrided materials showed S curve behavior with pulling rate. The reduction in fracture toughness is due to a localized deformation between axial splits.

9) A. K. Bind, et al [18]:-In this study Fracture toughness parameters of double melted cold worked and stress relieved Zr-2.5Nb Pressure tube material and helium quenched from 843, 873 and 903 °C were evaluated as a function of hydrogen content (20-100 wppm). For as received sample,  $K_Q$  increases with increase in hydrogen content and it value saturates at 100 ppm. For other samples  $K_Q$  was observed to decrease with increase in hydrogen content. The magnitude of slope of  $J_{max}$  and  $dJ/da$  of all heat-treated samples were greater than received samples and is maximum for samples helium quenched from 873 °C and decreased drastically after that. At 25 °C autoclaved material showed marginal increase in fracture toughness with increase in hydrogen content. The samples treated at 873 °C showed highest toughness value. The alloy treated at 903 °C was observed to be less susceptible to hydride embrittlement.

- 10) R.N. Singh, et al [19]:-A FEM was used to compute the stress field of precipitation and dissolution hydride for fully constrained and semi-constrained cases using material property of hydride and matrix at 25, 200 and 400 °C. Hydride expansion and matrix contraction simulation were carried out in order to simulate hydride precipitation and dissolution. Matrix interface during expansion was tensile while the same for dissolving hydride was compressive.
- 11) Priti Kotak Shah, et al [27]:-In this study tensile properties of double-melted as well as quadruple melted Zr-2.5 Nb pressure tubes were tested on around 50 pressure tube off-cuts in longitudinal and transverse tensile direction. Miniature flat tensile specimens having 1.8 mm width and 1.5 mm thickness and 7.6 mm gauge length were prepared without flattening treatment. The specimens showed higher yield strength (YS) and ultimate tensile strength (UTS) compared to the longitudinal specimens. Transverse specimens showed less strain hardening compared to the longitudinal specimens. The axial specimens showed higher uniform (UE) and total elongation (TE) compared to the transverse specimens. Double-melted pressure tubes showed relatively higher strength and lower elongation and larger standard deviation compared to the quadruple melted pressure tubes. In general the transverse specimens showed higher yield strength (YS) and ultimate tensile strength (UTS) compared to longitudinal specimens. Transverse specimens showed less strain hardening compared to the longitudinal specimens. The axial specimens showed higher uniform (UE) and total elongation (TE) compared to the transverse specimens. The tensile properties at 300°C for longitudinal and transverse

are given as YS (MPa) 440,530. UTS (MPa) 568, 605. UE (%) 4.6, 1.9. TE (%) 21.5, 16.2.

- 12) V. Srikanth, et al [33]. The residual stresses developed in the material between roll joint were estimated using FEM analysis for SS304L / Zr-2.5%Nb joints. The maximum and minimum values of normal stresses  $\sigma_{xx}$  and  $\sigma_{yy}$  were found to act on SS and Zr-2.5%Nb part, respectively near the joint interface. The maximum tensile stress  $\sigma_{xx}$  acting in radial direction on SS part was found to decrease from 260 MPa to 243 MPa due to Ni Ti interaction. Minimum compressive stress acting on Zr-2.5%Nb side was found to reduce from 315 MPa to 290 MPa. Compression stress  $\sigma_{yy}$  acting on Zr-2.5%Nb in axial direction also found to reduce from 92 MPa to 55 MPa.

The objective of this study was to study the influence of hydrogen content (more than 200 wppm) on FT of Zr-2.5Nb alloy having radial hydride. The CANDU and Indian PT fabrication process is similar but not the same and many studies are done by CANDU pressure tube. However fracture properties of the CANDU pressure tube are not representative of the Indian pressure tube due to difference in microstructure and overall fabrication process [28]. Several studies have been performed for the Zr-2.5Nb alloy having circumferential hydride [2,4,7,9,10,17,18] to calculate the effect of hydrogen on FT. Also studies have been performed to calculate the FT with the variation of HCC that is hydrogen continuity coefficient at different temperature [4, 9,15,29]. The fracture toughness for radial hydride contain 100wppm hydrogen for CWSR Zr-2.5Nb PT have been studies [2,4]. The studies on flatten specimen of an irradiated Zircaloy-2 PT material for CANDU reactor for HCC values of 0.5 FT of CANDU pressure tube has been reported in paper[30].

However fracture behavior of Zr-2.5Nb pressure tube is different upon both HCC and hydrogen contain which are not systematically



investigated, although they are required for the safety assessment of PT in working life. All of these studies were performed on PT material having hydrogen content less than 100 wppm and also most of the paper is studied on HCC from 0 to 0.56[2,4,7,9,10,17,18,28,29,30] where HCC zero represent 100% circumferential hydrides and one represent 100% radial hydrides. Recent studies present the effect of stress oriented hydrides on DHC velocity of Zircaloy-4 cladding material[28]. Various degree of PT hydride can develop as a result of improper rolling, accidental cooling under high pressure, blister formation oxide nodule formation presence of crack it is etc[26]. Due to continuous corrosion reaction, temperature gradient and stress gradient, hydrogen diffuses towards cold spot and higher stress and may reach values greater than 200 wppm locally[26]. Because of these it is important to study the FT having radial hydride for more than 200 wppm hydrogen wppm hydrogen. I have not found any study in open literature for FT having radial hydrides for more than 200 wppm of Indian pressure tube. Zr-2.5Nb alloy. That's why it is also important to study the effect of radial hydride on the FT of pressure tube having more than 200 wppm hydrogen.

## Chapter 3

### Material And Method

#### Chapter 3.1

#### Material Specification

The pressure tube of Indian pressurized heavy water reactor is made in Nuclear Fuel Complex in Hyderabad. It follows the procedure similar to AECL ( Atomic Energy of Canada Limited) modified route 2. But the process is not same. The following process is followed at NFC Hyderabad for making PT. From the quadruple melted ingot Zr-2.5Nb is subjected to  $\beta$  quenching from 1000 °C after soaking for half hour. The ingot gives 3 billets. That is top, middle and bottom. The billet is subjected to extrusion process of extrusion ratio 8 : 1 at temperature of 800°C. After that it is vacuum stress relieved for 3 hour at 480 °C after that it follows first stage of cold pilgering 50-55%. Then it is vacuum annealed 550 °C for 6 hours followed by second stage of cold pilgering 20 to 25 percent. [24]. Flow chart for this process is shown in figure 4.

Element in Zr-2.5Nb	Specific Value Quadruple Melted
Niobium, %	2.5
Oxygen, ppm	900-1300
Iron, ppm	650 max
Hydrogen, ppm	5 max
Chlorine, ppm	0.5 max
Phosphorous, ppm	10 max

Table 1. Composition of quadruple melted pressure tube. [27]

The material used in this study is cold worked and stress relieved CWSR Zr-2.5Nb used for the Indian 220MWe PHWR reactor. The PTs are made by quadruple melted ingots followed by hot extrusion with two stage pilgering and an intermediate annealing. The initial hydrogen content of the PT was about 5wppm. The composition [27] is shown in table. A section of about 450mm length was cut from the full length PT.

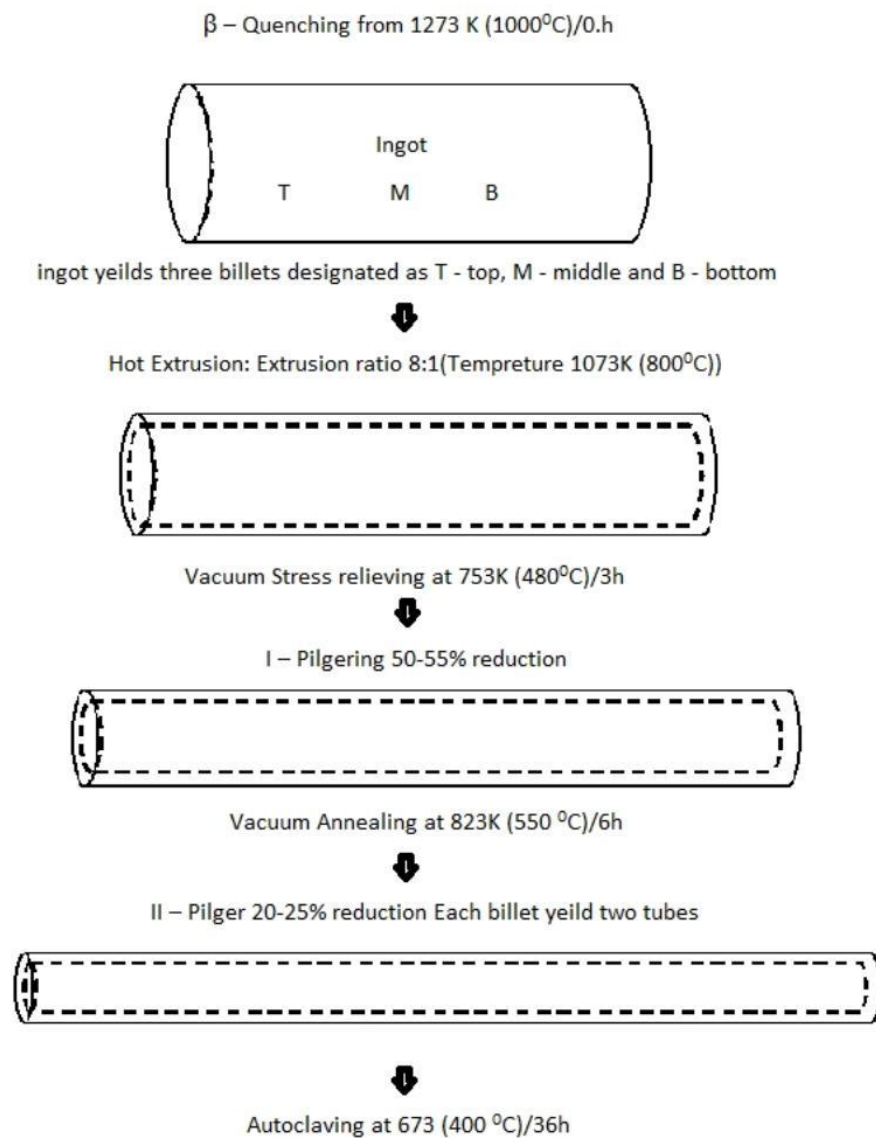


Fig.4. Step wise representation of manufacturing of pressure tube in NFC Hyderabad according to Modified AECL route 2 of Indian standard.[16]

## Chapter 3.2

### Hydrogen Charging

A 450mm length was cut from the full length PT. The PT section was then gaseously charged with hydrogen using the modified Sieverts apparatus[25]. When a metal is exposed to hydrogen gas, it can absorb and retain a certain amount of hydrogen in solution. In gaseous hydrogen charging technique Zr-alloy samples are heated in hydrogen atmosphere in a constant volume system. In the constant volume system, the average hydrogen concentration of the sample is estimated from the product of system volume and the difference between the initial and final pressure of the system. In this technique, the samples can be hydrided completely i.e. the amount of hydrogen charged is not limited to the terminal solid solubility of hydrogen in the alloy.

For charging, first the oxide layer formed due to the oxidation of Zr in atmosphere is to be removed. The PT section was polished using silicon carbide grinding wheel to remove the oxide layer from inner and outer surfaces of the PT section. Sample is then kept in isolated furnace and air in the furnace is pumped out using a vacuum pump. The vacuum pump was started and vacuum upto  $1 \times 10^{-4}$  Torr was obtained. After evacuating the furnace chamber, hydrogen is released into it and furnace is switched on to heat till  $363^\circ\text{C}$ . Hydrogen gas starts to expand due to increasing temperature, which results in increase in pressure. Finally, at a particular point pressure start to decrease as hydrogen starts to diffuses into sample. Pressure in the furnace drops as hydrogen gets diffused. Required Amount of hydrogen concentration can be obtain using the weight of sample which is weighed before putting it in furnace and required dropped in pressure which is estimated after the pressure reaches its peak.

The amount of hydrogen charged can be calculated from the universal gas law.

$n = \Delta PV/RT$  which gives number of moles of hydrogen.

Wt. of hydrogen =  $2n$

$[H] \text{ ppm} = \text{wt of hydrogen} \times 10^6 / \text{wt of spool}$

Where  $\Delta P$  is difference between initial and final partial pressures,  $T$  is temperature,  $wt$  is weight,  $R$  is universal gas constant and  $V$  is volume of the internal charging system. Hence the required drop in the partial pressure gives the hydrogen content.

### Chapter 3.3

#### Formation of Radial Hydrides

An experimental setup was designed, fabricated and used to form radial hydrides in Zr-2.5Nb alloy pressure tube spool. The design of setup was based on ensuring a hoop stress in the spool greater than the threshold stress [16] for reorientation of hydrides in this alloy while cooling from solution annealing temperature, which was achieved by application of internal pressure [2,6].

The experimental setup can be pressurized up to 25MPa and more than 300°C temperature. Minimum flow of the water medium was achieved through natural convection phenomenon to get uniform temperature along the PT length and circumference. A pressurized accumulator is provided in the loop. The accumulator facilitates to maintain the constant pressure throughout the stress reorientation process [16]. Following procedure was followed for the radial hydride formation:

1. Mounting of PT spool rolled into end fitting flanges on both sides to the experimental setup.
2. Heating of the PT spool to 400°C temperature at minimum possible pressure for 30mins.
3. Cooling the PT spool to 350°C and soak for 30mins.
4. Increasing the pressure inside the PT spool to the corresponding hoop stress greater than the threshold stress [20] for radial hydride formation and soaking for 30mins.
5. Cooling of the PT spool at the rate of ~1°C/min to 150°C and maintaining the constant pressure for 30 min inside PT spool.
6. Again heating the PT spool at constant pressure to 350°C and soaking 30 min.
7. Repeating the step 5 and step 6 for 10 thermal cycles.
8. Releasing the pressure and cooling the PT to room temperature.

Three thermocouples each at both ends and one at middle of the PT section were mounted to monitor the temperature along the tube section axis.

## Chapter 3.4

## Pre-Cracking

The curved compact specimen of 17 millimeter width is made from spool of Zr-2.5Nb tube as per the standards of ASTM E-1820-13. The dimension of the specimen is shown in figure 5b. The hydride and stress oriented specimen are directly cut from the spool using a wire electron discharge machining.

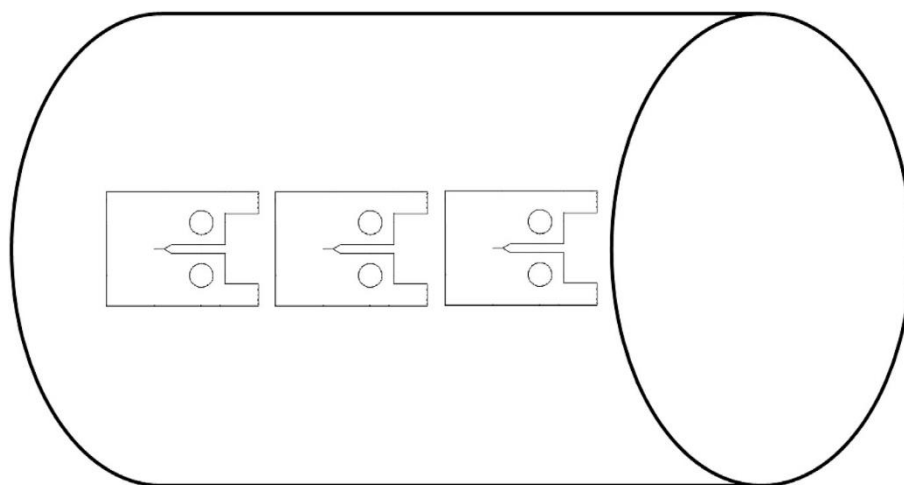


Fig.5.a. CCT sample cut from PT spool .

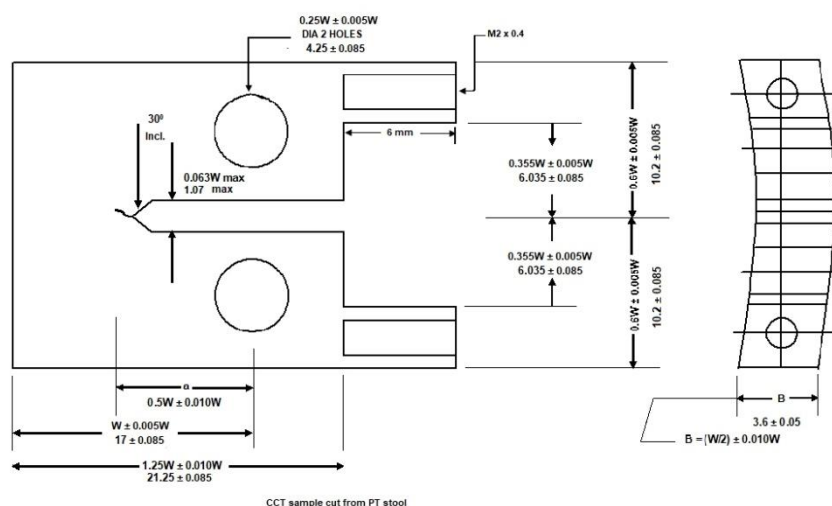


Fig.5.b. CCT sample specification and dimensions. [1]

The machining of CCT specimen was carried out such that the crack plane was set along the axial radial plane and direction of crack propagation is along axial direction of Spool .To obtain the sharpest possible crack tip all the samples are precracked on a Rumul Make Resonance Fatigue Machine in a four successive stage by fatigue precracking. The process consists of four stages of amplitude 450 N, 400 N, 350 N, 300 N with load ratio of 0.2 and a decrease in stress intensity factor with each successive stage. The static load applied was 50 Newton. the total size of the pre crack will be such that  $a / W \sim 0.5$

The interface software name is rumul test lab. Tapered pin is used for precrack as the sample is curved so that true and uniform front cracks form, instead of crack only on one side.



## Chapter 3.5

### Experimentation

The fracture toughness test was carried out on a UTM Zwick Roell Kappa 100 DS machine. The sample was held in place on UTM between clevis grips with the help of two pins for mod 1 fracture test . a voltage moderator Instek power supply is connected to the test sample using screw and copper wire to supply a constant current of 6A. The platinum wire of diameter 0.2 mm welded on either side of crack opening notch that is the flat surface of the test specimen shown in figure 5b. the platinum wire is used for recording the direct current potential drop (dcpd) of the specimen with the crack growth.

At initial stage the voltage recorded by the unfractured specimen is near to 3mV. Three K type thermocouple are connected to top and bottom attachment and one to specimen to calculate the temperature of the specimen. Electric resistance furnace is used to raise the temperature of the specimen to the test temperature using programmed controller. The furnace is started and the specimen is heated in air at the rate of 5 °C / min. After reaching the test temperature the specimen is allowed to soak at that temperature for 1 hour. After 1 hour the UTM starts and tensile displacement is applied at constant rate of 0.2 mm / min.

The online monitoring of the load, load line displacement and dcpd is done by the software testxpert for mode 1 tensile fracture test of specimen. After reaching a decrease in 40% of maximum load, the machine stops and the specimen is removed from the UTM. The experiment is repeated for 7 test temperature RT, 150 ,225, 250, 262, 275 and 300°C.



Fig 6. UTM Zwick Roell Kappa 100DS

## Chapter 3.6

### Pre-Crack Length Calculation

The fractured sample is analyzed under stereo microscope. Pre cracked and fractured surface images of all samples were taken from the stereo microscope. Using imagej software and stereographic microscope image, the average crack length of each sample is calculated using 9 point average method [2]. In this method 5% distance of precracked thickness is left on both side along the thickness correspond to the flat surface of precrack. Two lines are drawn parallel to the length of precrack at this two points on both side of the thickness. Now 7 lines parallel to the precrack length are drawn between these two lines at equal distance from each other. Distance from starting of pre crack to the precracked front along this lines represent the length of precrack which can be easily seen from the stereographic image. The length of these lines are calculated from line 1<sup>st</sup> to line 9<sup>th</sup> that is L1,L2,---L9. Now the average of line 1<sup>st</sup> and line 9<sup>th</sup> is taken and then average of this length and remaining 7 lines are taken. The length obtained is the average length of pre crack.

Similar method is used to calculate the total fracture length corresponding to the thickness of the fractured surface.

## Chapter 3.7

### Metallographic Analysis

For metallographic analysis the samples were cut in in RC plane and then polished for etching. The polishing is done using silicon carbide paper of FEPA standard in increasing grit size of 200, 500, 800, 1000. The etching is done using Kroll's reagent that is 45%  $\text{HNO}_3$ , 45%  $\text{H}_2\text{O}$ , 10%  $\text{HF}$  for few seconds by rubbing a cotton ball soaked in reagent on the surface. The microscopic images revealed presence of 100% radial hydrides figure (7-13). RC plane images for sample at all test temperature are given below.

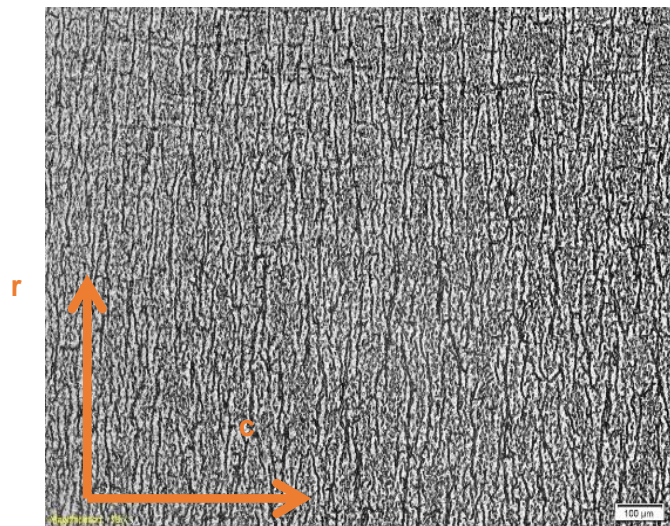


Fig 7. Optical microscope image of RC plane for test temperature 300°C.

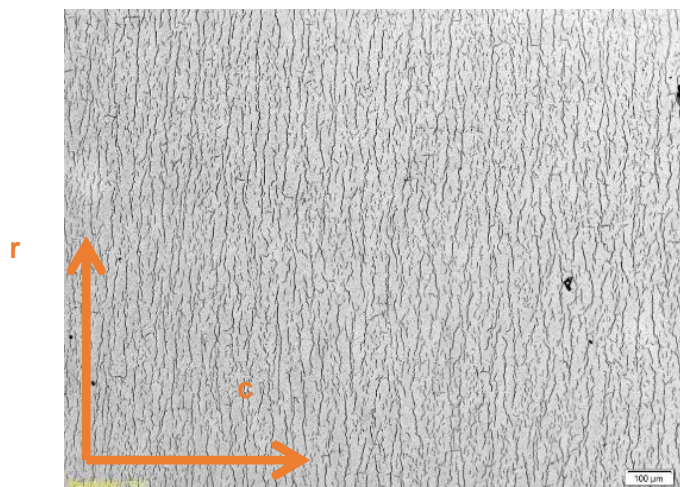


Fig.8. Optical microscope image of RC plane for test temperature 275°C

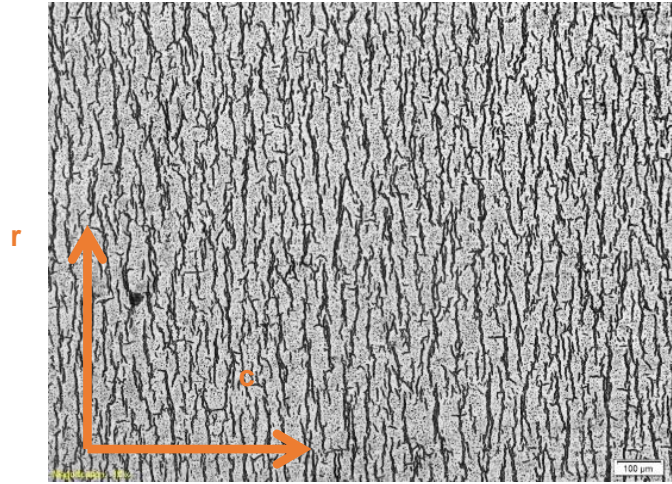


Fig.9. Optical microscope image of RC plane for test temperature 262°C

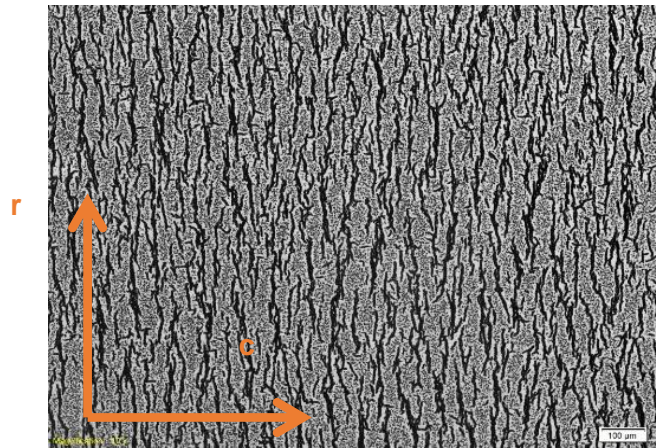


Fig.10. Optical microscope image of RC plane for test temperature 250°C.

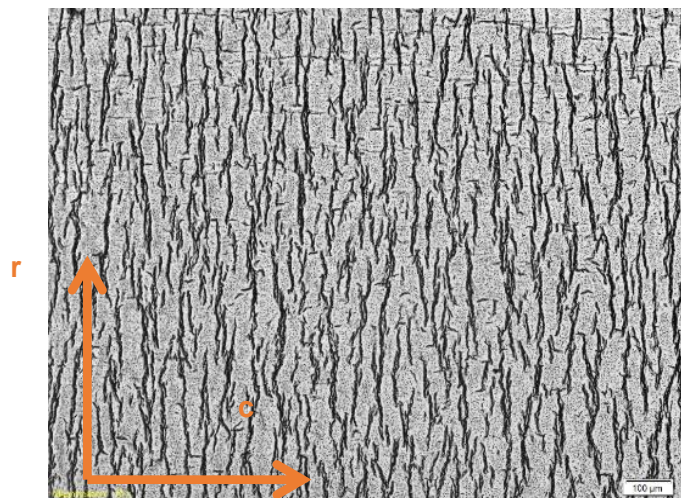


Fig 11 Optical microscope image of RC plane for test temperature 225°C



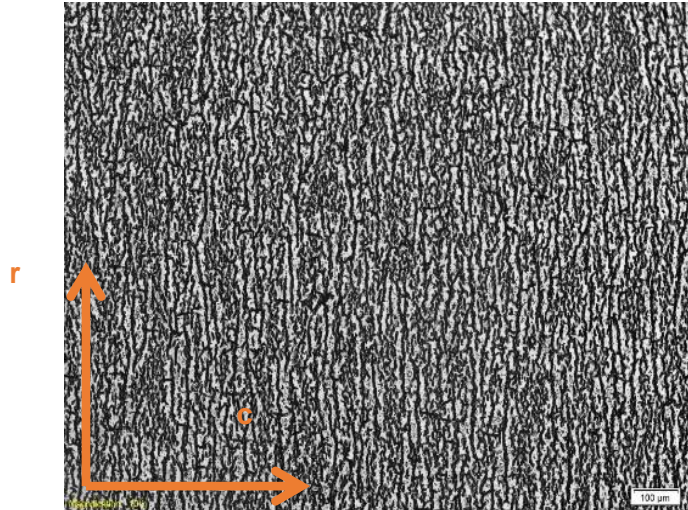


Fig.12. Optical microscope image of RC plane for test temperature 150°C

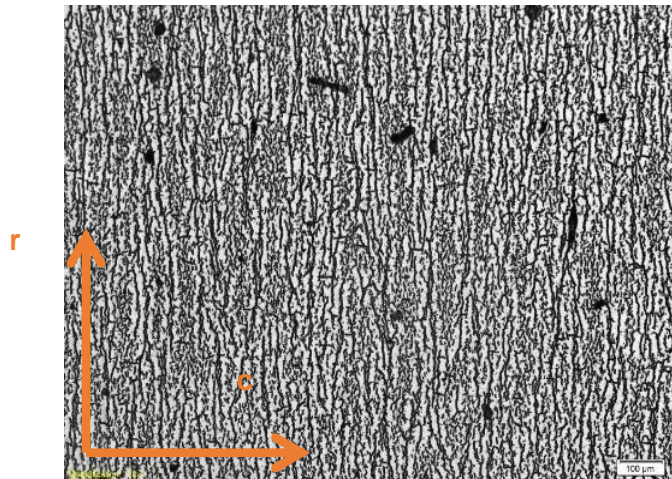


Fig.13. Optical microscope image of RC plane for test temperature 25°C

## Chapter 3.8

### Hydrogen Content Analysis

Small pieces of hydrogen charged samples were sliced manually by using slow speed cut-off wheel. The weight of the samples should be from 100 mg to 70 mg. After slicing, the samples were thoroughly washed with acetone to remove any dirt or trace of coolant oil using ultrasonic cleaning. Finally all these samples were analyzed for their hydrogen content by inert gas fusion technique[25]. About 1.5 g tin granules as flux were taken in a graphite crucible. The system was degassed at 700-850 A, and then set to analyze with a current of 650 A. The blank reading was taken and then the sample to be analyzed was dropped in to the crucible. High purity argon was used as the carrier gas. Calibration standards were run in between. The evolved gases were passed through the dust trap to remove carbon particulates and then through Schultz reagent to oxidize CO to CO<sub>2</sub>. The CO<sub>2</sub> was trapped by ascarite column and the water formed was trapped by MgClO<sub>4</sub> column. The N<sub>2</sub> and H<sub>2</sub> gases were then separated by molecular sieve column and H<sub>2</sub> was determined by TC detector.

For RT sample the hydrogen content is 320wppm using inert gas fusion technique. Analysis of all optical images of RC plane using imagej software and comparing with RT sample hydrogen content indicates hydrogen content of all samples are within  $\pm 5\%$  RT.

## Chapter 3.9

### Fracture Toughness Analysis

Fracture toughness is the ability of material to resist failure by fracture. According to Griffith the fracture will not propagate unless the energy required for cracked to propagate is sufficient to overcome the material resistance. Rice shows that the energy release of a non-linear elastic or elastic plastic material can be represented as a line integral along a contour from one crack surface to other and encloses crack front, called as J integral. The energy release rate for a nonlinear material is represented by j integral. Experimentally it is calculated using the area under the load versus load line displacement. As per the ASTM standard E-1820-13, for calculating the fracture toughness of CCT sample we use the following formula  $J = J_{el} + J_{pl}$

where  $J_{el}$  represent elastic integral and  $J_{pl}$  represent plastic j integral. And it is calculated as by ASTM E-1820-13 [1] standards as.

$$J_{(i)} = J_{el(i)} + J_{pl(i)}$$

$$J_{el(i)} = \frac{(K_{I(i)})^2 (1 - \nu^2)}{E}$$

$$K_{I(i)} = \frac{P_{(i)}}{BW^{0.5}} f\left(\frac{a_{(i)}}{W}\right)$$

$$f\left(\frac{a_{(i)}}{W}\right) = \frac{\left[2 + \frac{a_{(i)}}{W}\right] \left[0.886 + 4.64 \frac{a_{(i)}}{W} - 13.32 \left(\frac{a_{(i)}}{W}\right)^2 + 14.72 \left(\frac{a_{(i)}}{W}\right)^3 - 5.6 \left(\frac{a_{(i)}}{W}\right)^4\right]}{\left(1 - \frac{a_{(i)}}{W}\right)^{\frac{3}{2}}}$$

$$J_{pl(i)} = \left[ J_{pl(i-1)} + \frac{\eta_{(i-1)}}{b_{(i-1)}} \frac{(A_{pl(i)} - A_{pl(i-1)})}{B} \right] \left[ \left(1 - \gamma_{(i-1)} \left| \frac{(a_{(i)} - a_{(i-1)})}{b_{(i-1)}} \right| \right) \right]$$

$$A_{pl(i)} - A_{pl(i-1)} = \frac{(P_{(i-1)} + P_{(i)})(V_{(i-1)} - V_{(i)})}{2}$$

$$\eta_{(i-1)} = 2 + \frac{0.522b_{(i-1)}}{W} , \quad \gamma_{(i-1)} = 1 + \frac{0.76b_{(i-1)}}{W}$$



Where,

$A_{pl(i)}$  = plastic area under load vs load line displacement curve.

$V_{pl(i)}$  = plastic part of the load-line displacement.

$P_{(i)}$  = load at i.

$a_{(i)}$  = crack length at i

W = Width of specimen.

B = net specimen thickness.

$b_o$  = uncracked ligament,  $(W - a_o)$ .

The Young's modulus and Poisson's ratio [7] with respect to temperature is given as  $E = 95900 - 57.4T$  Mpa,  $\nu = 0.436 - 4.8/10000 \cdot (T - 25)$ .

The quantity  $A_{pl(i)} - A_{pl(i-1)}$  is the increment of plastic area under the chosen force versus plastic displacement recorded between lines of constant plastic displacement of point corresponding to crack length  $a_{(i)}$  and  $a_{(i-1)}$

The procedure for calculating the  $J_{max}$  which is corresponding to the maximum load is calculated using the sigma plot software the procedure is as follows. The data of current, DCPD voltage, load line displacement, load, precrack length, total crack length, width, thickness, flow stress is loaded into the worksheet of sigma plot. Graph of load versus load line displacement is plotted to remove the initial curvature developed due to grip and pin adjustment which is done by plotting a linear regression line of all data points by superimposing on the graph. Initial data points are removed to obtain linear line of data points, the curvature obtained due to plastic crack extension is also adjusted to obtain final data points. Now only linear line is obtained which represents the elastic portion of CCT sample. Slope and load intercept is calculated of this line. The load vs. load line displacement data is shown in fig. (14-20). Using this load intercept and slope the load line displacement that is stroke is adjusted to match with origin[1]. Now the data points corresponding to the plastic portion which comes after the elastic linear line is loaded in 2<sup>nd</sup> worksheet with corrected stroke. The crack

extension increment is also evaluated using initial and final crack length and DCPD voltage by using linear interpolation. The initiation of crack is represented by the deviation of voltage of DCPD .After this compliance and corrected plastic stroke is calculated. Now the corrected plastic stroke and all the data necessary for calculating the J integral is loaded in worksheet 3. After this increment in plastic areas calculated and finally J elastic and J plastic is calculated as per the formula[1].

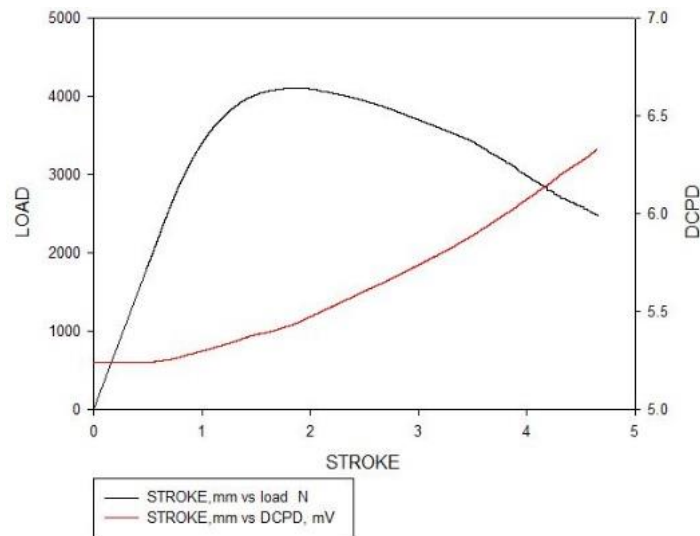


Fig.14. Load vs Load Line Displacement vs DCPD graph for test temperature 300°C

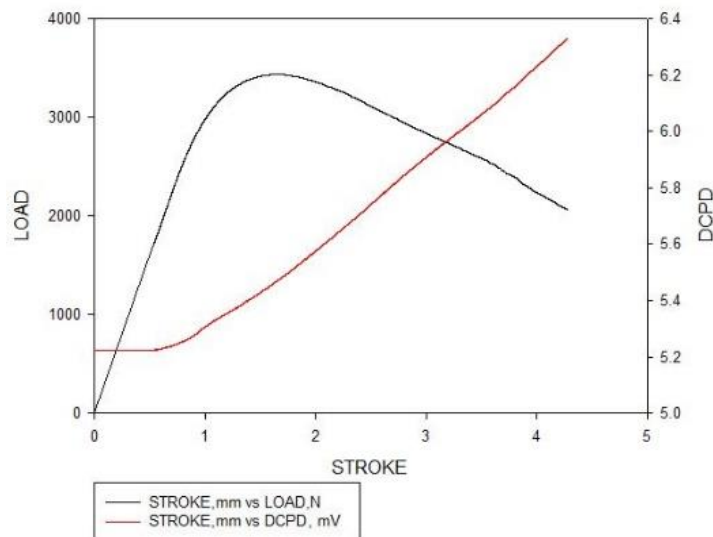


Fig.15. Load vs Load Line Displacement vs DCPD graph for test temperature 275°C

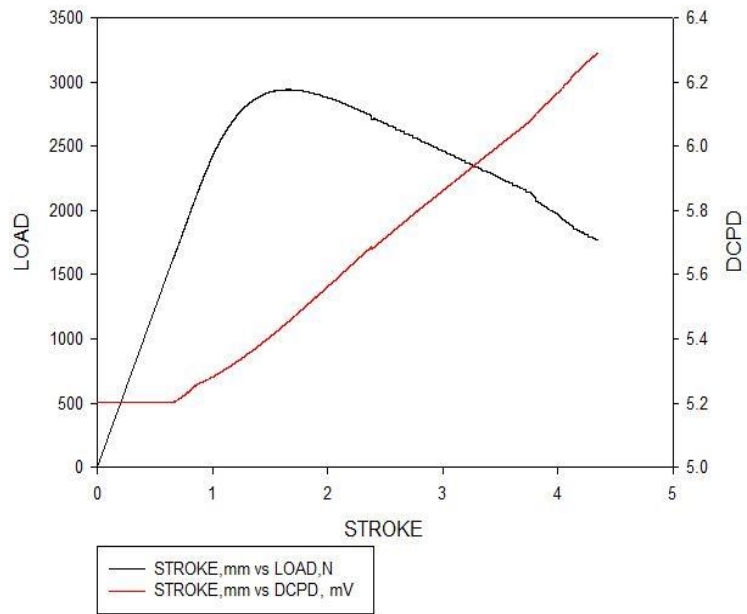


Fig.16.. Load vs Load Line Displacement vs DCPD graph for test temperature 262°C

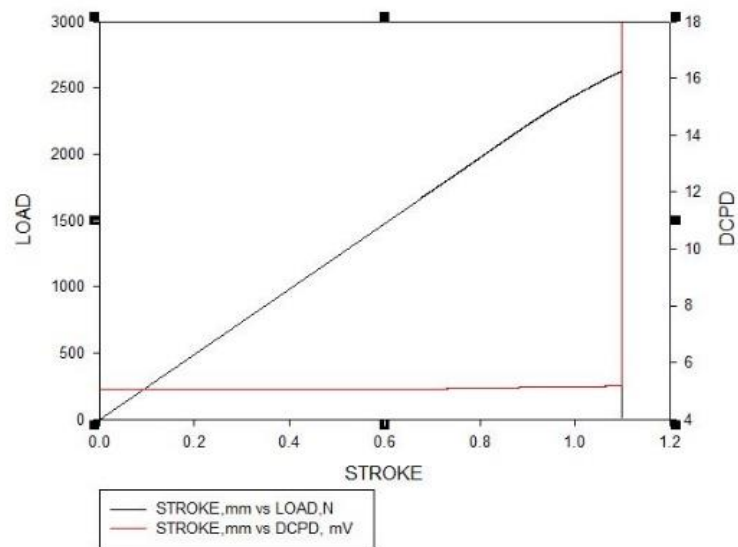


Fig.17. Load vs Load Line Displacement vs DCPD graph for test temperature 250°C.

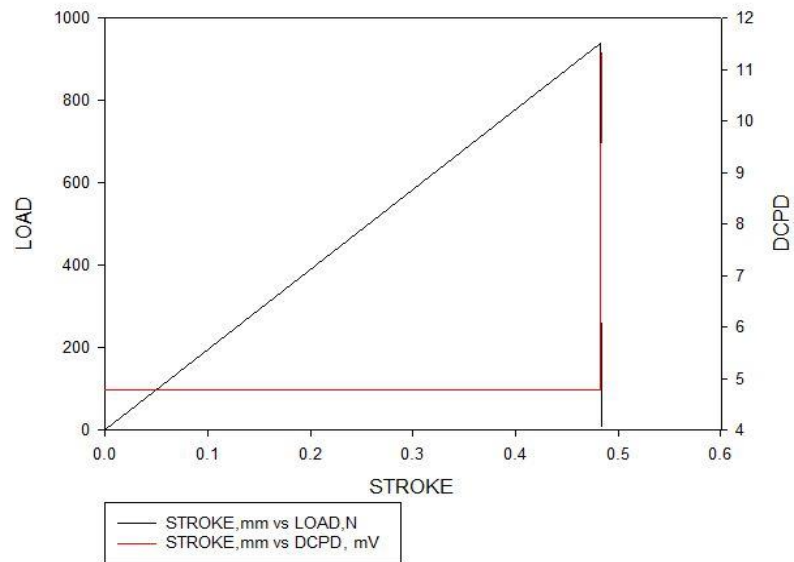


Fig.18. Load vs Load Line Displacement vs DCPD graph for test temperature 225°C.

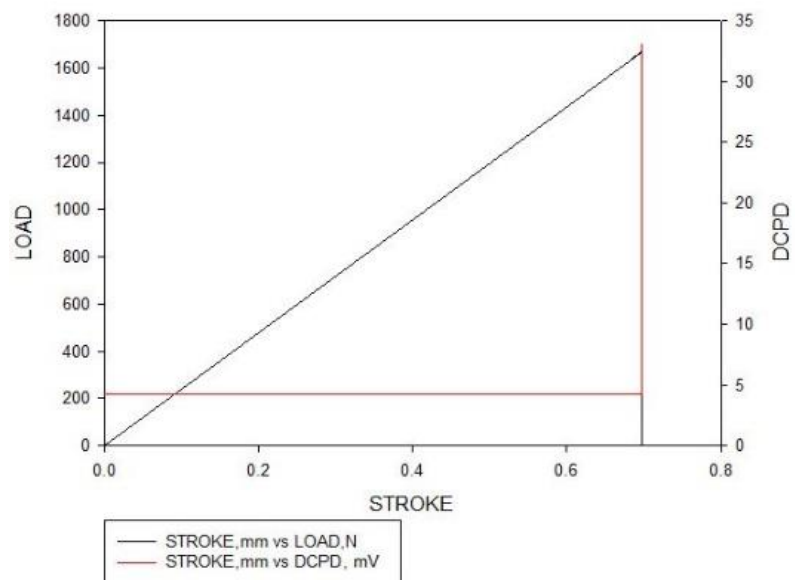


Fig.19. Load vs Load Line Displacement vs DCPD graph for test temperature 150°C

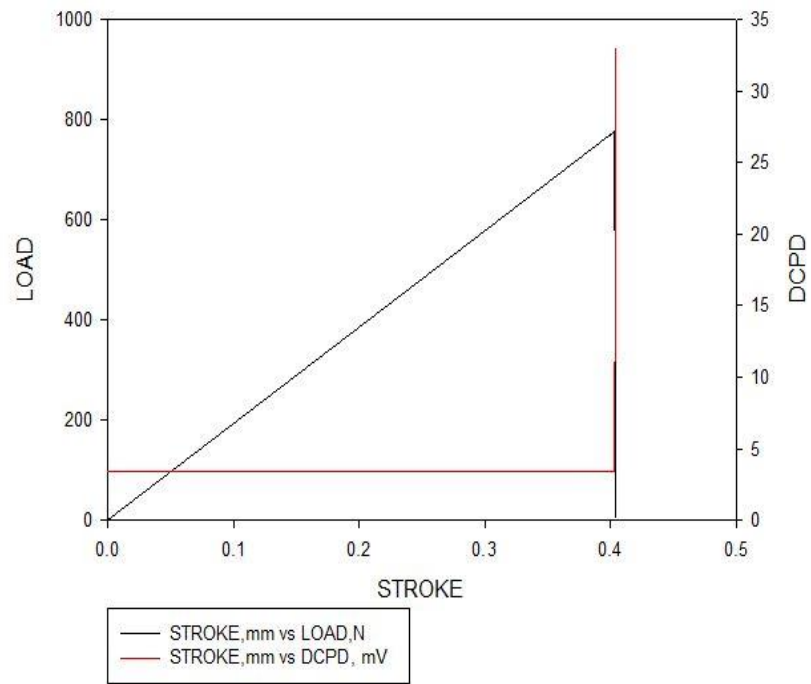


Fig 20. Load vs Load Line Displacement graph for test temperature 25°C

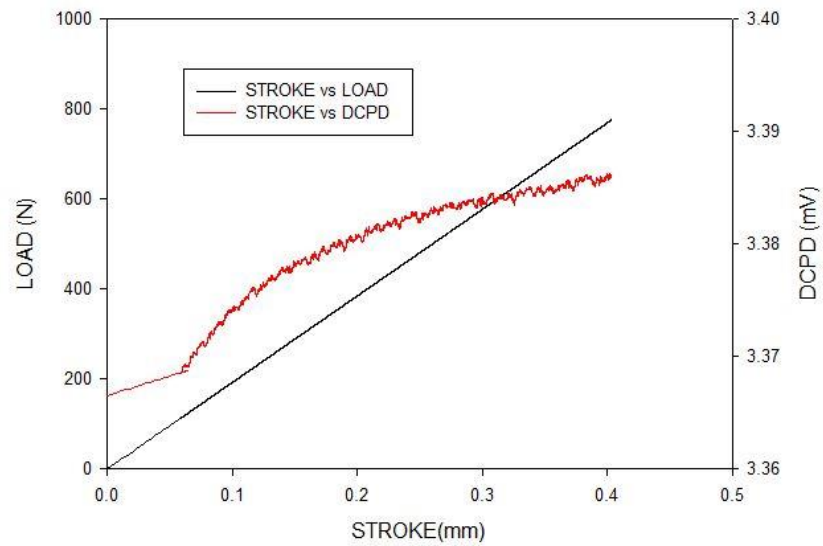


Fig.21. Load vs Load Line Displacement vs higher magnification of DCPD graph for test temperature 25°C.

## Chapter 3.10

### Critical Crack Length Analysis

The CCL is the length of crack above which unstable crack growth take place. LBB is a defense against the failure of the PT. Before complete failure of the PT, the heavy water leak out of a through crack form in the wall of PT. This leakage can be detected by detecting the change in moisture between PT and calendria tube. Precautions are taken and the tube which is going to fail is removed. This concept is called Leak Before Break. The minimum size of crack which shows leakage is taken as four times the thickness of tube according to the [6]. The CCL should be greater than the LLB length with a factor of safety of 2. The CCL is calculated for all test temperature and are shown in table.2. Following formula is used for calculating the CCL [14].

$$c = \frac{K_{max}^2 \pi}{8\sigma_f^2 \ln \left[ \sec \left( \frac{\pi M \sigma_h}{2\sigma_f} \right) \right]}$$

$$M = \left[ 1 + 1.255 \left( \frac{c^2}{r_m w} \right) - 0.0135 \left( \frac{c^2}{r_m w} \right)^2 \right]^{1/2}$$

$$\sigma_h = p \left( \frac{r_m - 0.5w}{w} + 1 \right)$$

Where,

Kmax = stress intensity corresponding to maximum load

C = CCL / 2

w= thickness of tube

$\sigma_f$  = flow stress.

$\sigma_h$  = hoop stress

P = pressure

$r_m$  = mean radius of tube

## Chapter 4

### Results And Discussion

The metallography images in RC plane shown in figure 7-13 which confirms presence of 100% radial hydride. In figure 31 shows J max versus temperature graph of four curves. The first three curves are the data from [2], showing the fracture toughness variation with the temperature for uncharged, 100wppm circumferential hydride and 100 wppm radial hydride. The last below curve shows the variation of fracture toughness with temperature for current thesis data that is for ~320wppm radial hydride. At the beginning of the curve for 320 wppm, the fracture toughness is 3 kJ/m<sup>2</sup> for room temperature. This shows that the resistance of material for crack propagation at room temperature is very low. Up to 225° C, data shows the increase in fracture toughness is negligible. We get almost flat region between 25°C and 225°C. Above 225°C, the fracture toughness starts to increase. As the hydride contained is high in the material (figure 33), we can conclude that the increase in fracture toughness is due to the increase in ductility of  $\alpha$ -Zr matrix, rather than dissociation of hydride into the material. We can see a sharp brittle to ductile transition between 250°C and 262°C. The fracture toughness jumps from 36 kJ / m<sup>2</sup> at 250°C to 145 kJ / m<sup>2</sup> at 262°C. From this we can conclude that the presence of radial hydride has significant deteriorating effect below to 262°C and formation of radial hydride should be avoided in pressure tube. The formation of radial hydride is not expected in CWSR Zr- 2.5Nb pressure tube material under normal operating condition but due to improper role joining operation internal stresses could be generated at joints and the total stress level could go beyond threshold stress of orientation[2]. From 262°C and above due to plastic deformation and increase in ductility, the fracture toughness increases significantly. At 300°C, the fracture toughness of 100 wppm radial hydride and 320wppm radial hydride and 100wppm circumferential hydride is almost close 207kJ / m<sup>2</sup>  $\pm$  15kJ / m<sup>2</sup>. which shows that at higher operating temperature the fracture

toughness is almost identical whether hydrides formed are circumferential or radial. In overall  $J_{max}$  versus temperature curve for 320 wppm have typical s- shape curve and the ductile to brittle transition is sharp between 250°C to 262°C. As compared to the 100wppm circumferential hydride graph from figure 31 we see that the brittle to ductile transition is gradual, therefore we can say that the susceptibility of fracture toughness with temperature in the presence of radial hydride is more. The overall curve for 320 wppm is shifted towards higher temperature and lower fracture toughness as compared to 100 wppm radial hydride. This is due to the presence of higher concentration of hydrogen in 320wppm. The fracture toughness of 320 wppm was found to be lower than the material with 100wppm circumferential hydrides at all test temperature, which suggest adverse effect of radial hydrides over circumferential hydrides.

The load vs load line displacement graph are shown in figure 14-20. The load vs load line displacement graph shown for test temperature 25°C, 150°C, 225°C, suggest brittle failure of sample as there is no deviation from linearity in fig 18-20. For 262°C and above we can clearly see that there is a ductile failure from the non-linearity of the curve, suggesting there is significant plastic deformation before failure. This indicates that crack propagation for ductile material is accompanied by significant plastic deformation which results in more dissipation of energy into the plastic zone and blunting of crack which eventually result in higher fracture toughness. At 250°C, we can see a little deviation from the linear line suggesting there is a little plastic deformation before complete failure of material which indicates starting temperature of brittle to ductile transition. Even if at room temperature the material behave like brittle, the DCPD vs load vs load line displacement from figure 21 for 25°C test temperature suggest a little crack growth before sudden failure.

The crack surface images taken for stereomicroscope are shown in figure 28-30 for test temperature of 25°C, 150°C and 225°C shows flat region and which confirm brittle failure. Stereo microscope images for



temperature 262°C, 275°C and 300°C show tearing of surface and also crimping at the outer surface along the thickness which suggest plastic deformation with crack growth figure 24-26 . So above 262°C, failure is ductile. Micro mechanism of crack growth can be suggested as axial splitting in axial-radial plane of hydrides along with the localized deformation of in between material ligaments. For 250°C test temperature sample shows somewhat flat region, but higher magnification is required to be confirm. Figure 27.

Figure 32 shows CCL vs temperature graph for more than 320 wppm radial hydride and uncharged PT data taken from [2]. Horizontal line is also taken which represent the LLB length with factor of safety 2 corresponding to the thickness of the pressure tube [6]. From the figure 32, it is clear that the pressure tube with CCL for temperature 250°C and above will indicate LLB and provide time for replacement of PT [6]. The CCL at test temperature 25°C, 150°C, 225°C is not safe as there will be no indication of leakage before reaching the critical length for unstable crack growth. Therefore precaution has to be taken during pressurizing at starting up of reactor, if radial hydrides are present.

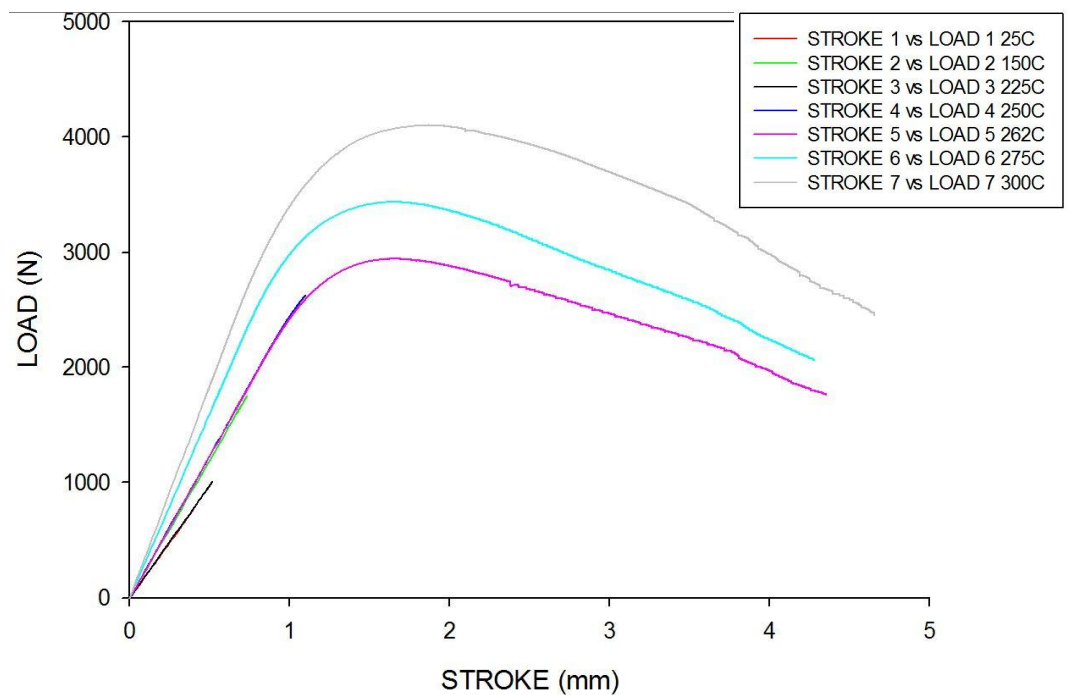


Fig.22. Load vs. load line displacement for all temperature range.

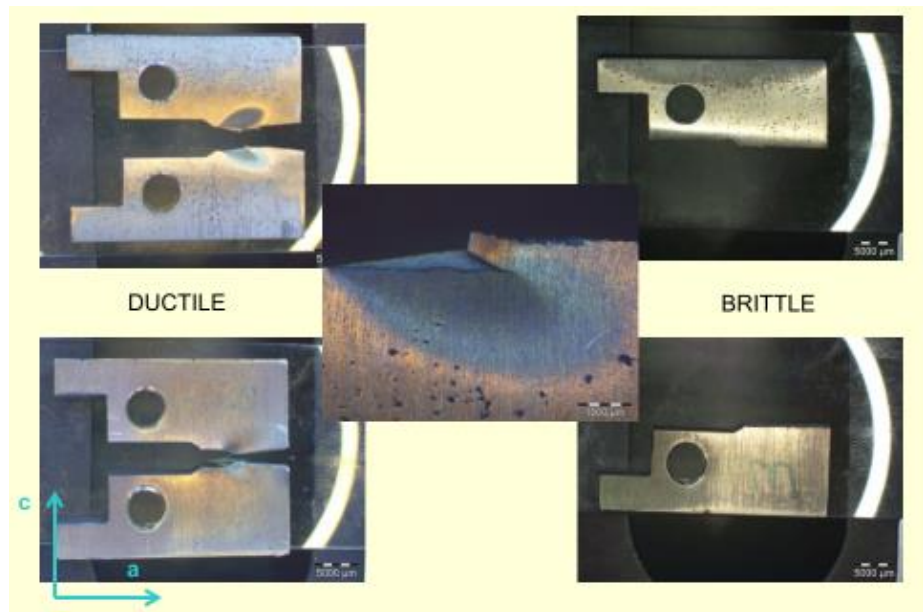


Fig.23. Front and back surface of CCT sample for ductile and brittle test sample

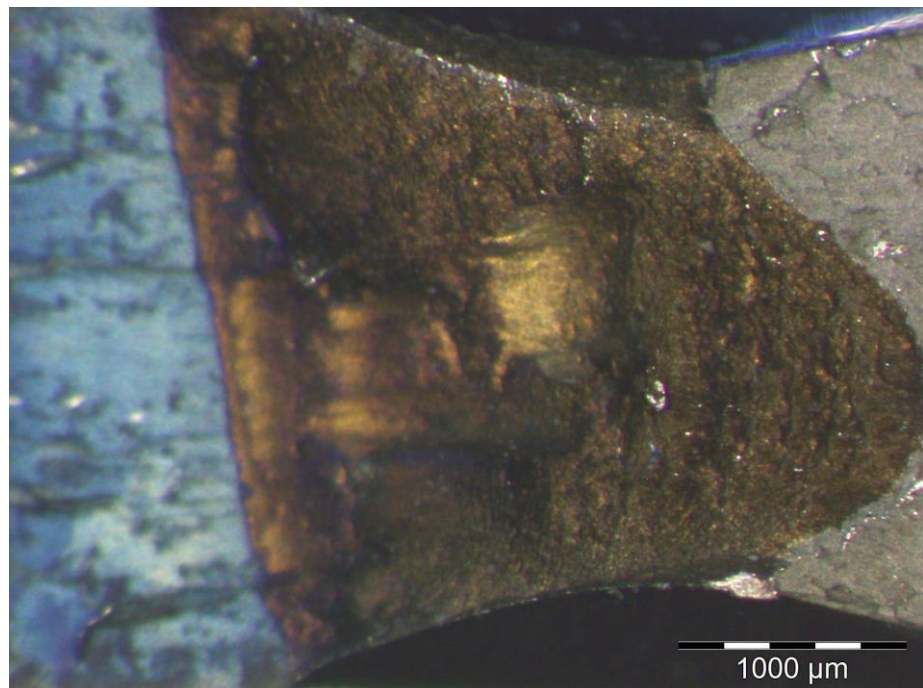


Fig.24. Stereo microscope image of crack surface after fracture testing for test temperature 300°C.

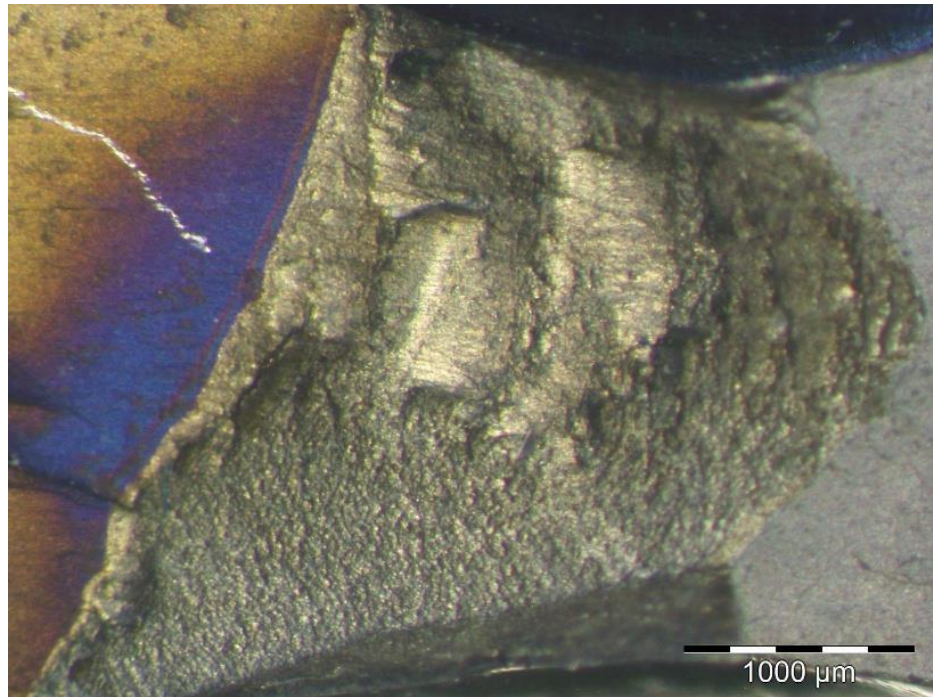


Fig.25. Stereo microscope image of crack surface after fracture testing for test temperature 275°C.

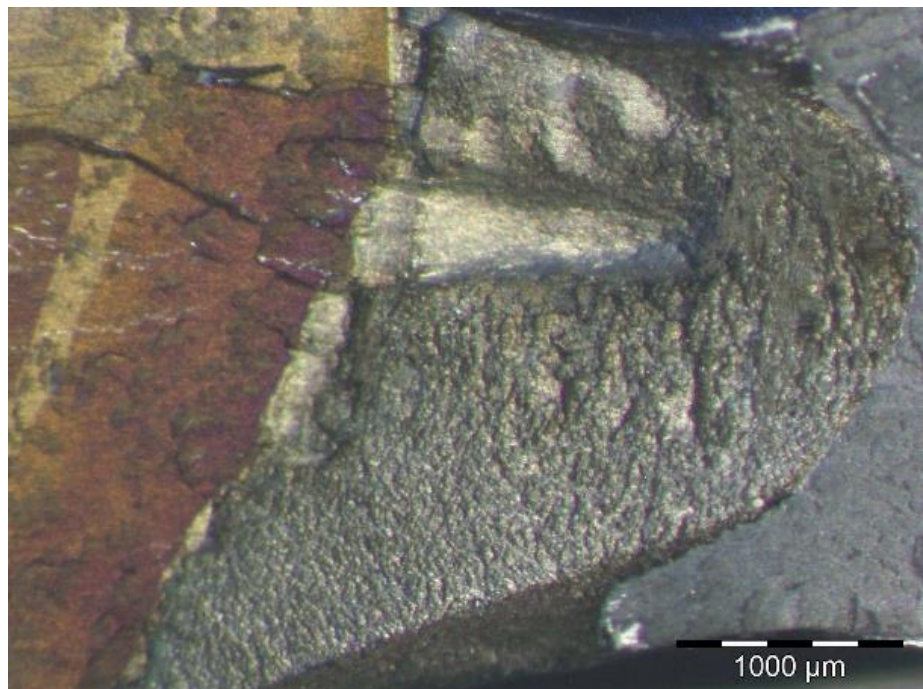


Fig.26. Stereo microscope image of crack surface after fracture testing for test temperature 262°C.



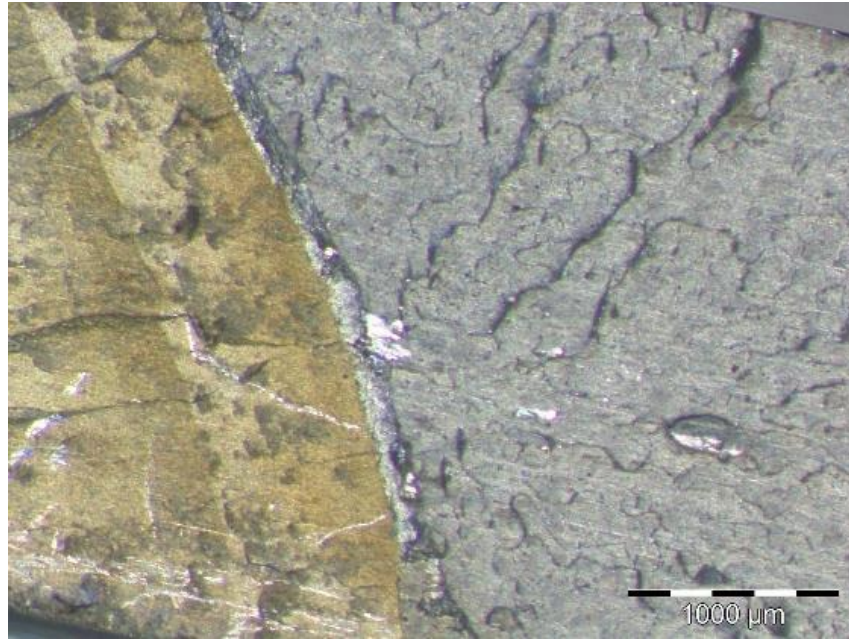


Fig.27. Stereo microscope image of crack surface after fracture testing for test temperature 250°C.

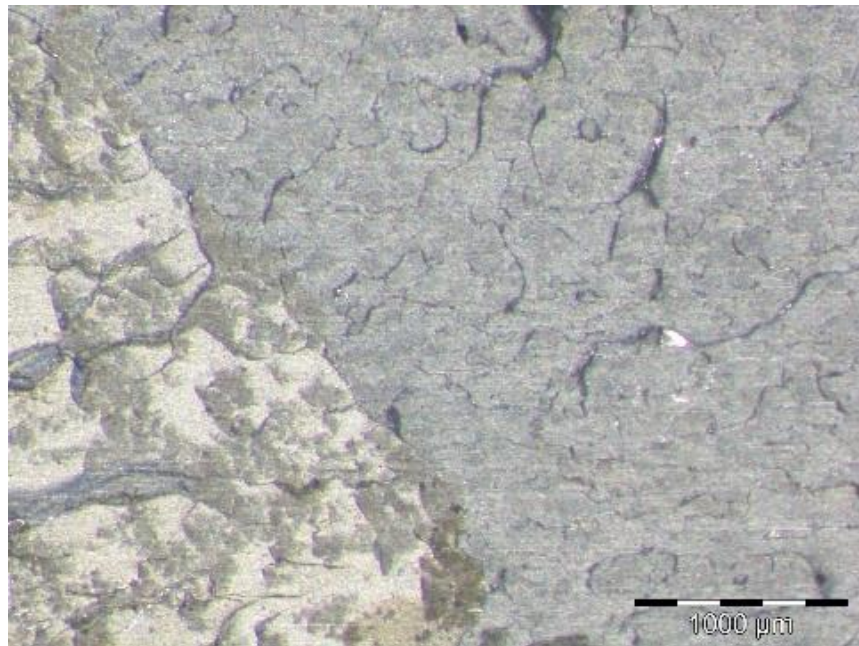


Fig.28. Stereo microscope image of crack surface after fracture testing for test temperature 225°C.

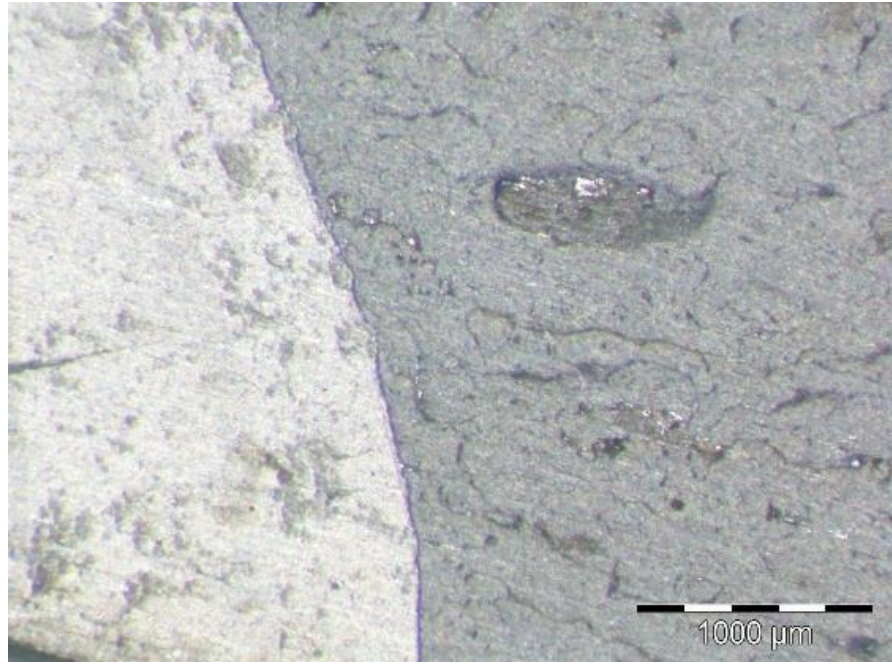


Fig.29. Stereo microscope image of crack surface after fracture testing for test temperature 150°C.

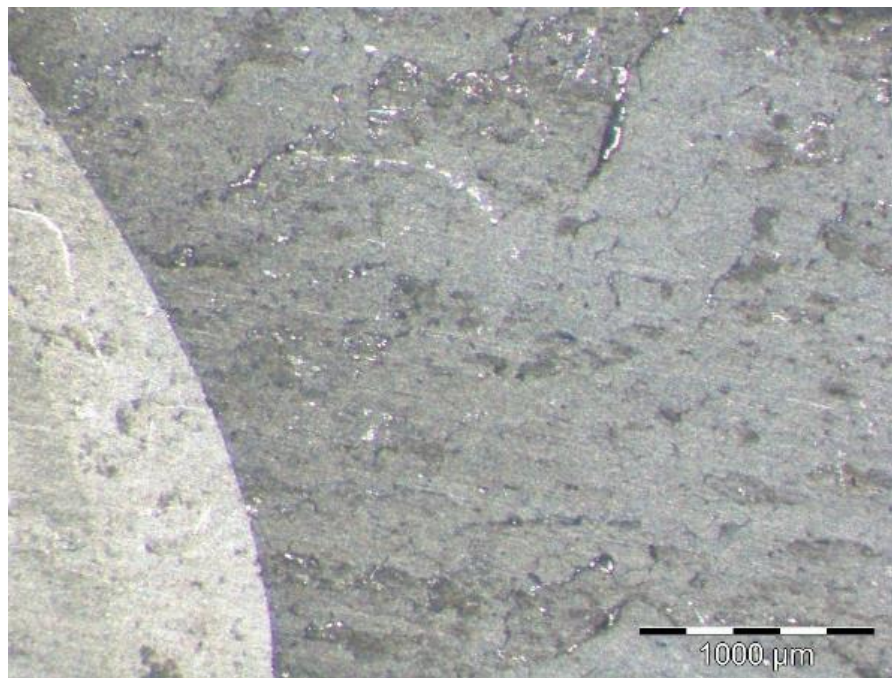


Fig.30. Stereo microscope image of crack surface after fracture testing for test temperature 25°C.



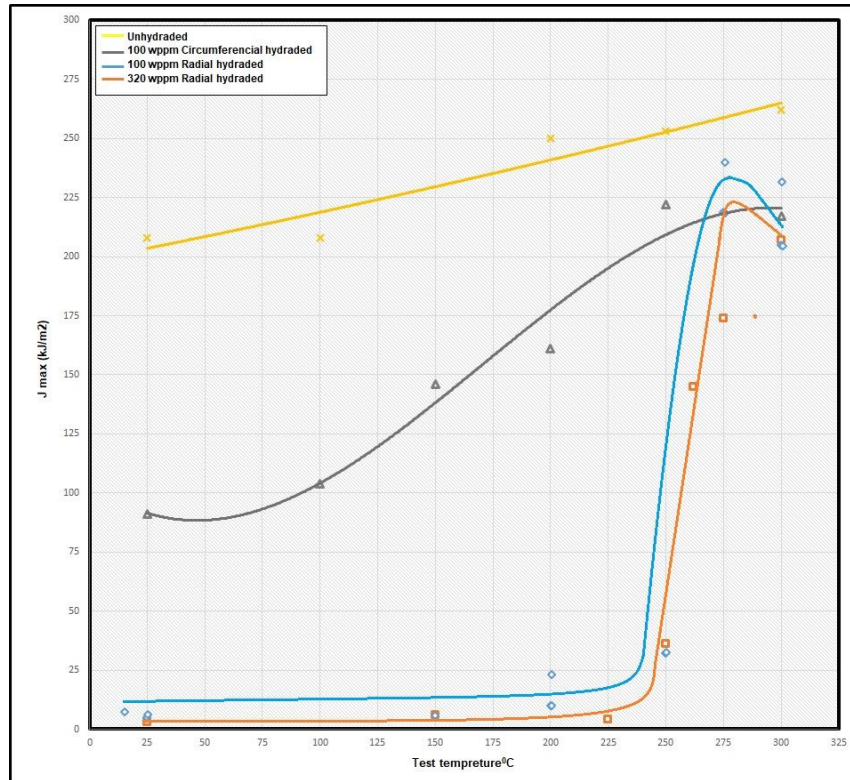


Fig.31.Jmax vs. temperature for more than 200 wppm radial hydride, along with comparison for unhydrided, 100 wppm circumferential hydrided and 200 wppm circumferentially hydrided taken from [2].

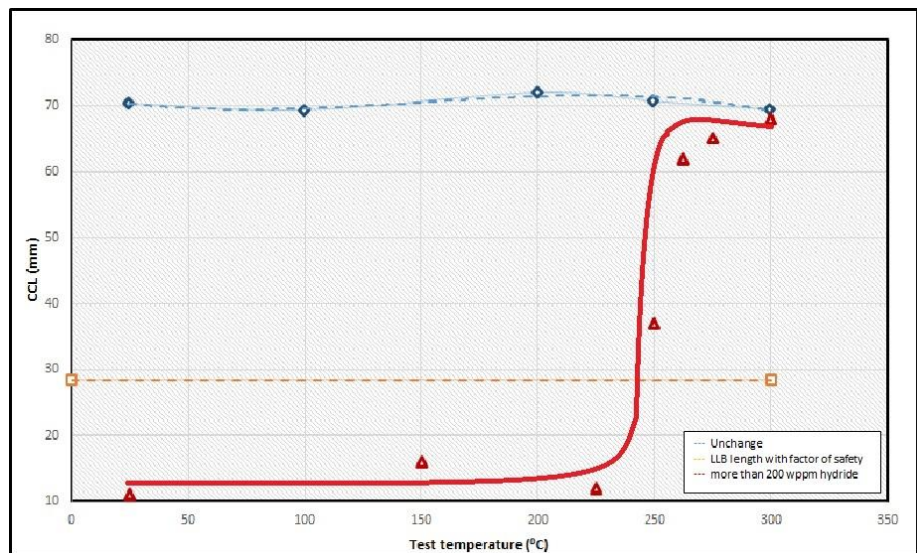


Fig.32. CCL vs Test Temperature for uncharged Zr-2.5Nb from [2], LLB crack length with factor of safety and for radial hydride having more than 200wppm hydrogen.

Sr.No	Temperature °C	Fracture Toughness KJ/m <sup>2</sup>	CCL mm
1	300	207	68
2	275	174	65
3	262	145	62
4	250	36	37
5	225	4	12
6	150	6	16
7	25	3	11

Table 2. Fracture Toughness and CCL calculation data of this thesis.

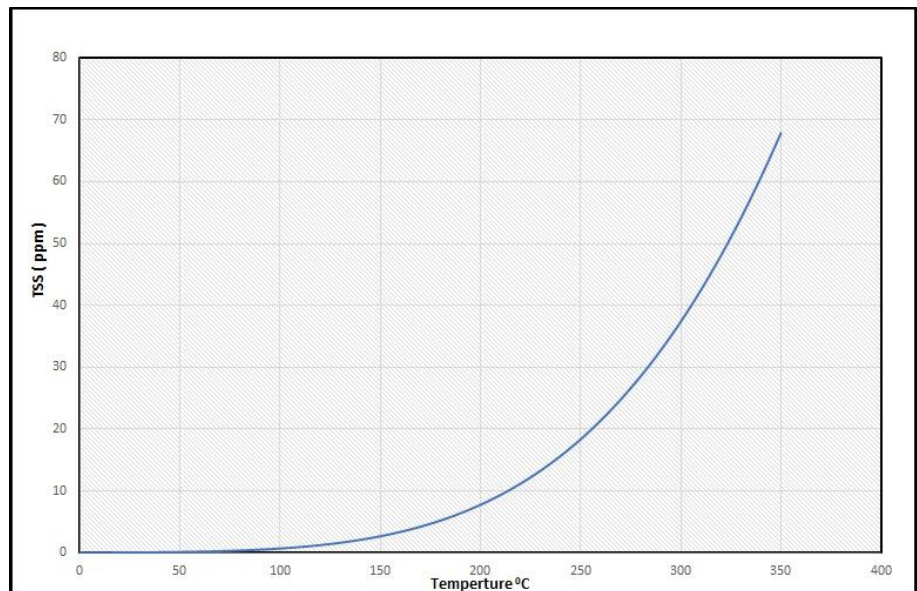


Fig.33. Graph of terminal solid solubility of dissolution verses temperature.[16]

## Chapter 5

### CONCLUSION

- 1) The effect of radial hydride on the fracture toughness of Zr-2.5Nb pressure tube containing 320 wppm hydrogen has been successfully studied.
- 2) The temperature dependency due to the presence of radial hydride can be significantly seen on the fracture toughness with a sharp increase in fracture toughness 250°C-262°C.
- 3) The fracture toughness of pressure tube material containing radial hydride 100 wppm and 320wppm radial hydride are near to  $\sim 207 \text{ kJ/m}^2$  at 300°C. which suggest at higher temperature, hydride orientation has less significance effect on fracture toughness.
- 4) The CCL versus Temperature graph shows that during active reactor temperature range i.e. above 250°C, crack will form which will have leakage before reaching its critical value.
- 5) The stereo microscope images show clear sign of ductile tearing and brittle flat surface for temperature between 25°C to 300°C.



## Chapter 6

### FUTURE DIRECTION

- 1) The hydrogen of the sample is conformed using imagej software with reference to the hydrogen content data of one sample. So, it is required to conform the hydrogen content of all samples using inert gas fusion technique.
- 2) Only stereo microscope image is analyzed. Unless we see the sem images, which will show the crack surface at higher magnification we cannot conform the micro mechanism of crack growth. For 320wppm of hydride at 300°C, the terminal solid solubility is ~65wppm. So there is still a high quantity of hydride present during fracture testing at 300°C. So it is necessary to conform the micromechanics of crack growth using sem.
- 3) During fracture testing of Zr-2.5Nb pressure tube material having 320wppm radial hydride at low temperature, the metallographic analysis of axial circumferential plane shows bending of hydride near the initiation of crack. I have not found any reference related to bending of hydride. The metallographic images suggest that the hydrides flow with the material. This phenomenon has to be studied further.

## REFERENCES

- [1] ASTM-Standards, Standard Test Method for Measurement of Fracture Toughness, 2013. ASTM E-1820.<https://www.astm.org/Standards/E1820>
- [2] R.K. Sharma, S. Sunil, B.K. Kumawat, R.N. Singh, A. Tewari, B.P. Kashyap, Influence of hydride orientation on fracture toughness of CWSR Zr-2.5%Nb Pressure tube material between RT and 300 C, J. Nucl. Mater. 488 (2017) 231-244. <https://doi.org/10.1016/j.jnucmat.2017.03.025>.
- [3] Bourga R, Moore P, Janin Y-J, Wang B, Sharples J, Leak-Before-Break: Global perspectives and procedures, International Journal of Pressure Vessels and Piping (2015), doi: 10.1016/j.ijpvp.2015.02.004.
- [4] Rishi K. Sharma , A.K. Bind , G. Avinash , R.N. Singh , Asim Tewari , B.P. Kashyap.(2018).Effect of radial hydride fraction on fracture toughness of CWSR Zr-2.5%Nb pressure tube material between ambient and 300 °C temperatures. <https://doi.org/10.1016/j.jnucmat.2018.06.003>
- [5] R.K. Sharma, A. Tewari, R.N. Singh, B.P. Kashyap, Optimum shape and orientation of  $\delta$ -hydride precipitate in  $\alpha$ -Zirconium matrix for different temperatures, Journal of Alloys and Compounds (2018), doi: 10.1016/j.jallcom.2017.12.085.

[6] G.D. Moan, C.E. Coleman, E.G. Price, D.K. Rodgers, S. Sagat, Leak before break in the pressure tubes of CANDU reactors, *Int. J. Pres. Ves. Pip.* 43 (1990) 1-21. [https://doi.org/10.1016/0308-0161\(90\)90089-Z](https://doi.org/10.1016/0308-0161(90)90089-Z).

[7] R.N. Singh, A.K. Bind, N.S. Srinivasan, P. Stahle, Influence of hydrogen content on fracture toughness of CWSR Zr-2.5Nb pressure tube alloy, *J. Nucl. Mater.* 432 (2013) 87-93. <https://doi.org/10.1016/j.jnucmat.2012.07.046>.

[8] K.S. Chan, X. He, Y.M. Pan, Fracture resistance of a Zirconium alloy with reoriented hydrides, *Metall. Mater. Trans.* 46 (1) (2015) 58-71. DOI: 10.1007/s11661-014-2225-1

[9] Jun Cui and Gordon K. Shek , .Effects of Hydride Morphology and Test Temperature on Fracture Toughness of Zr-2.5Nb Pressure Tube Material(2009).Proceedings of the ASME 2009 Pressure Vessels and Piping Division C July 26-30, 2009, Prague, Czech Republic.PVP2009-77260, pp. 81-96; 16 pages.

[10] L.A. Simpson, C.D. Cann, Fracture toughness of Zirconium Hydride and its Influence on the crack resistance of Zirconium alloys, *J. Nucl. Mater.* 87 (1979) 303-316. ([https://doi.org/10.1016/0022-3115\(79\)90567-1](https://doi.org/10.1016/0022-3115(79)90567-1))

[11] R.N. Singh, P. Stahle, J.K. Chakravarttya, A.A. Shmakov.(2009).Threshold stress intensity factor for delayed hydride cracking in Zr–2.5%Nb pressure tube alloy. *J Materials Science and Engineering*. <https://doi.org/10.1016/j.msea.2009.05.066>

[12] S. Sagat , C.K. Chow, M.P. Puls , C.E. Coleman.(2000).Delayed hydride cracking in Zirconium alloys in a temperature gradients. Journal of Nuclear Materials. [https://doi.org/10.1016/S0022-3115\(99\)00265-2](https://doi.org/10.1016/S0022-3115(99)00265-2)

[13]. D.O. Northwood, I.M. London, L.E. Bahen. Elastic Constants Of Zirconium Alloys. Journal of Nuclear Materials 55 (1975) . DOI: 10.1016/0022-3115(75)90071-9.

[14] CSA-N285.8-10, Technical Requirements for In-service Evaluation of Zirconium alloy Pressure Tubes in CANDU Reactors, D.13.3, Canadian Standard Association, 2010.

[15] Shun-ichi HONDA. FRACTURE TOUGHNESS OF Zr-2.5 wt% Nb PRESSURE TUBE( 1984 ). Nuclear Engineering and Design 81 (1984) 159-167 159 North-Holland, Amsterdam. [https://doi.org/10.1016/0029-5493\(84\)90003-7](https://doi.org/10.1016/0029-5493(84)90003-7)

[16] R.N. Singh, S. Mukherjee, A. Gupta, S. Banerjee, Terminal solid solubility of Hydrogen in Zr-alloy pressure tube materials, J. Alloys Compd. 389 (1-2) (2005) 102-112. <https://doi.org/10.1016/j.jallcom.2004.07.048>.

[17] A.K. Bind, R.N. Singh, H.K. Khandelwal, S. Sunil , G. Avinash, J.K. Chakravartty, P. Ståhle. Influence of loading rate and hydrogen content on fracture toughness of Zr-2.5Nb pressure tube material. Journal of Nuclear Materials 465 (2015) 177-188. <https://doi.org/10.1016/j.jnucmat.2015.05.050> .

[18] A. K. Bind, R. N. Singh, J. K. Chakravartty. Influence Of Hydrogen Content On Fracture Toughness Of Heat-Treated Zr-2.5Nb Alloy. (2013). Conference: SMiRT-22, At San Francisco, California, USA.

[19] R.N. Singh, H.K. Khandelwal, A.K. Bind, S. Sunil, P. Ståhle, Influence of stress field of expanding and contracting plate shaped precipitate on hydride embrittlement of Zr-alloys, Mater. Sci. Eng. A 579 (2013) 157-163. <https://doi.org/10.1016/j.msea.2013.04.117>.

[20] R.N. Singh, R. Lala Mikin, G.K. Dey, D.N. Sah, I.S. Batra, P. Ståhle, Influence of temperature on threshold stress for reorientation of hydrides and residual stress variation across thickness of Zr-2.5Nb alloy pressure tube, J. Nucl. Mater. 359 (3) (2006) 208-219. <https://doi.org/10.1016/j.jnucmat.2006.09.004>.

[21] V. PEROVIC, G.C. WEATHERLY. THE NUCLEATION OF HYDRIDES IN A Zr-2.5 wt% Nb ALLOY. (1984). Journal of Nuclear Materials 126 (1984) 160-169 North-Holland. Amsterdam. [https://doi.org/10.1016/0022-3115\(84\)90086-2](https://doi.org/10.1016/0022-3115(84)90086-2).

[22] R.N. Singh, R. Kishore, S.S. Singh, T.K. Sinha, B.P. Kashyap, Stress-reorientation of hydrides and hydride embrittlement of Zr-2.5 wt% Nb pressure tube alloy, J. Nucl. Mater. 325 (1) (2004) 26-33. <https://doi.org/10.1016/j.jnucmat.2003.10.009>.

[23] R.N. Singh, S. Roychowdhury, V.P. Sinha, T.K. Sinha, P.K. De, S. Banerjee, Delayed hydride cracking in Zr-2.5Nb pressure tube material: influence of fabrication routes, Mater. Sci. Eng. 374 (1-2) (2004) 342-350. <https://doi.org/10.1016/j.msea.2004.03.008>.

[24] R.N. Singh, S. Mukherjee, R. Kishore, B.P. Kashyap, Flow behavior of a modified Zr-2.5wt%Nb pressure tube alloy, J. Nucl. Mater. 345 (2-3) (2005), 146-161. <https://doi.org/10.1016/j.jnucmat.2005.05.008>.

[25] R.N. Singh, R. Kishore, S. Mukherjee, S. Roychowdhury, D. Srivastava, T.K. Sinha, P.K. De, R. Kameswaran, S.S. Sheelvantra, B. Gopalan, S. Banerjee, Hydrogen Charging, Hydrogen Content Analysis and Metallographic Examination of Hydride in Zirconium Alloys, 2003. BARC report E034. <https://inis.iaea.org> RN:39004710

[26] D.O. Northwood, U. Kosasih, Hydrides and delayed hydrogen cracking in Zirconium and its alloys, Int. Met. Rev. 28 (2) (1983) 92-121. DOI: 10.1179/imtr.1983.28.1.92.

[27] Priti Kotak Shah ,J.S. Dubey , D. Datta , R.S. Shriwastaw , B.N. Rath , R.N. Singh, S. Anantharamanb, J.K. Chakravarttyc. Tensile strength of Zr-2.5 Nb pressure tubes: A statistical study.(2015).<http://dx.doi.org/10.1016/j.nucengdes.2015.07.019>.

[28] V. Grigoriev, A.M.A. Holston, G. Lysell, D. Schrire, L. Hallstadius, S.T.Mahmood, I.Arimescu, Experimental Study of DHC of Unirradiated and Irradiated Fuel Cladding and Implications to In-pile Operation and Dry Storage Conditions, Zirconium in Nuclear Industry, ASTM STP1543, 2013.

[29] P.H. Davies, C.P. Stearns, Fracture toughness testing of Zircaloy-2 pressure tube material with radial hydrides using direct current potential Drop, fracture mechanics, ASTM STP 905 (1986) 379-400.(DOI:10.1520/STP17408S).

[30] A.C. Wallace, G.K. Shek, O.E. Lepik, Effects of hydride morphology on Zr-2.5Nb. Fracture toughness, zirconium in the nuclear industry, ASTM STP 1023 (1989) 66-88.

[31] Kwai S. Chan. An assessment of delayed hydride cracking in zirconium alloy cladding tubes under stress transients.(2013) International Materials Reviews 58(6):349-373. DOI: 10.1179/1743280412Y.0000000013.

[32]. Y. Pushpalatha Devi , H. Donthula , N. Keskar , Apu Sarkar , Kumar Vaibhaw, K.V. Mani Krishna.(2020).Microstructural evolution in (in alpha and beta Zr) region of Zr-2.5 wt% Nb annealed at different temperatures: Effect on mechanical properties.Journal of Nuclear Materials 530 (2020) 151978.  
<https://doi.org/10.1016/j.jnucmat.2019.151978>.

[33] V.Srikanth, A.Laik Estimation of residual stresses developed in SS 304L / Zr-2.5%Nb joints.(2019).Procedia Structural Integrity Volume 14, 2019, Pages 952-956. <https://doi.org/10.1016/j.prostr.2019.07.076>.